

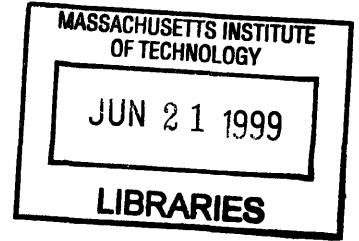
77

**AN EXPERIMENTAL METHOD FOR MEASURING
DYNAMIC PRESSURES ABOVE A CAVITATING
PROPELLER**

by

JACQUELINE BRENER KIRTLEY

B.S., Massachusetts Institute of Technology (1996)



SUBMITTED TO THE DEPARTMENT OF OCEAN ENGINEERING
IN PARTIAL FULFILLMENT OF THE REQUIREMENTS FOR THE DEGREE
OF

MASTER OF SCIENCE IN NAVAL ARCHITECTURE AND MARINE
ENGINEERING

at the

MASSACHUSETTS INSTITUTE OF TECHNOLOGY

September 1998

© Massachusetts Institute of Technology 1998. All rights reserved.

Author
Department of Ocean Engineering
September 2, 1998

Certified by
Justin E. Kerwin
Professor of Naval Architecture, Department of Ocean Engineering
Thesis Supervisor

Accepted by
J. Kim Vandiver
Professor of Ocean Engineering

An Experimental Method for Measuring Dynamic Pressures Above a Cavitating Propeller

by

Jacqueline Brener Kirtley

Submitted to the Department of Ocean Engineering
on September 2, 1998, in partial fulfillment of the
requirements for the degree of
Master of Science in Naval Architecture and Marine Engineering

Abstract

The basic objective of this project was to create an experiment and apparatus for measuring dynamic pressures above a cavitating propeller which could be used in modeling the differences between types of cavitation. A large, aluminum plate was designed to hold the pressure probes above the chosen 5 bladed surface ship propeller in an 5×5 array. The array of probes, along with upstream and downstream reference probes, acquired the dynamic pressures generated by the observed intermittent cavitations. Two computer applications were written to work with the apparatus: one for calibrating the pressure probes, and one for acquiring the data set of 20,000 samples per channel at 3,600 Hz. Contour plot animations and FFT analysis supported the experimental data and the experiment as a reusable apparatus for recording dynamic pressures to be used in cavitation computer models.

Thesis Supervisor: Justin E. Kerwin

Title: Professor of Naval Architecture, Department of Ocean Engineering

Acknowledgments

I would first like to thank Jake Kerwin for years of advice and help through this and my previous degree at MIT. I really do owe you for this chance to get my Masters degree and to be able to do this kind of physical testing—actually getting my hands wet.

I also owe a great deal to Richard Kimball for all of his assistance with this project and all of his know-how with so much of what I have done and worked on during my time at the Water Tunnel. Good luck completing your PhD and in everything to follow.

For their support and sponsorship, I would like to thank the University/Navy/Industry Consortium on Cavitation of High Speed Propulsors and its members: David Taylor Model Basin, Daewoo Shipbuilding & Heavy Machinery, El Pardo Model Basin, Hyundai Maritime Research Institute, KaMeWa AB, Michigan Wheel, Rolla SP Propellers SA, Sulzer-Hydro GMBH, Ulstein Propeller AS, Volvo-Penta of the Americas, and Wartsila Propulsion.

For all of their helpful assistance, insight, and at times materials and answers during this project, I would like to thank Spyros Kinnas of the Consortium on Cavitation Performance and the University of Texas at Austin, Scott Black of the David Taylor Model Basin, Peter Morley and Andrew Gallant from the MIT Central Machine Shop, and the Water Tunnel's very valuable UROPs Nicholas Hahn and Francisco Delatorre.

Lastly, I want to thank my family for their support, especially over my six years at MIT, and Jamez for everything.

Contents

1	Introduction	9
1.1	Cavitation Types	10
2	Designing the Experiment	11
2.1	The Propeller and the Plate	11
2.1.1	The Wake Screen	14
2.2	The Pressure Probes	14
2.2.1	Excitation Voltage and Wiring	17
2.2.2	The Differential Pressure Bladder	18
2.3	Data Acquisition System	18
2.3.1	Hardware	18
2.3.2	Software	19
3	Performing the Experiment	22
3.1	Installing the Plate	22
3.2	Installing the Pressure Probes	22
3.3	Running the Calibration Program	26
3.4	Running the Experiment	28
3.4.1	Take Data	29
3.4.2	Graph	30
3.4.3	Output to File	30
3.5	Processing Data	32
4	Experimental Results	33
4.1	Cavitation Conditions	33
4.2	Dynamic Pressure Output	35
4.3	Discussion and Improvements	54

4.3.1	Experimental Setup	54
4.3.2	Experimental Program	56
A	Two-Dimensional Foil Cavitation Experiment	57
B	Fortran and Matlab Programs	61
B.1	Matlab Calibration Program	61
B.2	Fortran Post-Processing Program	62
C	FFT Analysis of Dynamic Pressure Measurements	64
	Bibliography	71

List of Figures

2-1	The DTMB Propeller 4842	12
2-2	Drawing of Aluminum Experimental Plate	13
2-3	Tecplot ^(R) Contour of Non-Uniform Flow Field	15
2-4	Calibration Water Column from CAPREX III Experiment	16
3-1	Aluminum Strips for Arranging and Holding Pressure Probes onto the Ex- perimental Plate	23
3-2	Numbering Scheme for Pressure Probes	24
3-3	Pin Diagram for STP-100 and DAS-1801 HC	25
3-4	Photograph of PVC Bladder Setup and Location	26
3-5	On-screen Panel View of the <i>ChannelCheck</i> application	27
3-6	On-Screen Panel View of the <i>Experiment</i> Application	29
4-1	Photograph of Experimental Run A	34
4-2	Photograph of Experimental Run B	34
4-3	Photograph of Experimental Run C	35
4-4	Photographs of Experimental Run D from Both Sides of the Test Section .	36
4-5	Photographs of Experimental Run E from Both Sides of the Test Section .	37
4-6	Photograph of Experimental Run F	38
4-7	Photograph of Experimental Run G	38
4-8	Photographs of Experimental Run H from Both Sides of the Test Section .	39
4-9	Photograph of Experimental Run L	40
4-10	Photograph of Experimental Run M	40
4-11	Photograph of Experimental Run N	41
4-12	Photograph of Experimental Run O	41
4-13	Tecplot ^(R) Contour Plot for One Blade Passage of Run A	43
4-14	Tecplot ^(R) Contour Plot for One Blade Passage of Run B	44

4-15	Tecplot ^(R) Contour Plot for One Blade Passage of Run C	45
4-16	Tecplot ^(R) Contour Plot for One Blade Passage of Run D	46
4-17	Tecplot ^(R) Contour Plot for One Blade Passage of Run E	47
4-18	Tecplot ^(R) Contour Plot for One Blade Passage of Run F	48
4-19	Tecplot ^(R) Contour Plot for One Blade Passage of Run G	49
4-20	Tecplot ^(R) Contour Plot for One Blade Passage of Run H	50
4-21	Tecplot ^(R) Contour Plot for One Blade Passage of Run L	51
4-22	Tecplot ^(R) Contour Plot for One Blade Passage of Run M	52
4-23	Tecplot ^(R) Contour Plot for One Blade Passage of Run N	53
4-24	Tecplot ^(R) Contour Plot for One Blade Passage of Run O	55
A-1	Experimental Cavitation Map for the HRA Two-Dimensional Foil	58
A-2	Photograph of Bubble Cavitation on the HRA Two-Dimensional Foil at Cavitation Number $\sigma = 0.488$ and Angle of Attack $\alpha = 2^\circ$ with Camera Shutter Speed at $\frac{1}{2000}$ seconds	60
A-3	Photograph of Bubble Cavitation on the HRA Two-Dimensional Foil at Cavitation Number $\sigma = 0.488$ and Angle of Attack $\alpha = 2^\circ$ with Camera Shutter Speed at $\frac{1}{500}$ seconds	60
C-1	FFT Analysis for Run A, Blade Passage Frequency at 58.9 Hz	65
C-2	FFT Analysis for Run B, Blade Passage Frequency at 59.0 Hz	65
C-3	FFT Analysis for Run C, Blade Passage Frequency at 58.7 Hz	66
C-4	FFT Analysis for Run D, Blade Passage Frequency at 58.8 Hz	66
C-5	FFT Analysis for Run E, Blade Passage Frequency at 58.7 Hz	67
C-6	FFT Analysis for Run F, Blade Passage Frequency at 58.3 Hz	67
C-7	FFT Analysis for Run G, Blade Passage Frequency at 58.3 Hz	68
C-8	FFT Analysis for Run H, Blade Passage Frequency at 57.9 Hz	68
C-9	FFT Analysis for Run L, Blade Passage Frequency at 57.1 Hz	69
C-10	FFT Analysis for Run M, Blade Passage Frequency at 56.9 Hz	69
C-11	FFT Analysis for Run N, Blade Passage Frequency at 56.9 Hz	70
C-12	FFT Analysis for Run O, Blade Passage Frequency at 56.8 Hz	70

List of Tables

1.1	The Definitions of Different Cavitation Types as Used in CAPREX IV . . .	10
2.1	Pressure Probe Calibration Test By $\frac{Pressure}{RPM^2}$ as a Constant	17
3.1	Steps to Install the Aluminum Plate	23
3.2	Steps for Running the Calibration Application	28
3.3	Steps for Running the <i>Experiment</i> Application	31
4.1	Advance Ratio and Cavitation Number for Each Experimental Run	42

Chapter 1

Introduction

The main objective of this project was to create an experiment and apparatus for measuring dynamic pressures above a cavitating propeller. As the fourth phase in continuing work known as CAPREX, CAVitation PPropeller EXperiment, this project, CAPREX IV, was a reworking of the previous phase, CAPREX III, which had been unable to get reliable data[7]. Both CAPREX III and CAPREX IV were meant to create data sets for use in computer modeling of cavitation in a non-linear, uniform flow field.

Intermittent propeller cavitation has been a primary source of vibration on the hull of a ship. In the last few decades, the increased load on propellers brought out the cavitation generated ship vibrations due to propeller induced forces. Theoretical and experimental methods have studied and quantified these effects[2] which have been used in full-scale ship designs, as in [1]. Through the years, computer models, such as MIT-PUF-3A, have been developed to try to predict cavitation levels. More recently, an optimization code which infoprporated PUF-3A has been desinged to modify the propeller geometry based on a specific extent of cavitation[10]. These codes have been successful modeling and predicting leading edge sheet cavitation. Unfortunately, they have not been as successful with other types of cavitation, including mid chord, bubble, and tip vortex cavitation. To improve the computer programs so they include these additional cavitation types, data was needed to create models that could predict the different cavitation types.

To sufficiently model these intermittently cavitating propellers, the dynamic pressures caused by the propeller had to be resolved including the second and third harmonics of the blade rate, where propeller affects on ship vibrations have increased drastically due to cavitation. The data must also cover a planar area perpendicular to the propeller large enough to show the effects from the entire blade simultaneously.

Cavitation Type:	Definition:
Bubble Cavitation	A grouping of many small cavity bubbles appearing separated on the suction side surface of a foil. Bubble Cavitation may need a strobe light for clear visualization or else it appears to be a turbulent series of cavitation streaks.
Hub Vortex Cavitation	A cylindrical cavity following downstream of and created by the propeller hub.
Leading Edge Sheet Cavitation	A cavity on the suction side of a foil with inception at the leading edge of the blade. Sheet cavitation has a mirror-like surface sometimes containing streaks.
Midchord Cavitation	Any cavity, sheet or bubble, with inception at a mid-chord point on the blade.
Tip Vortex Cavitation	A ribbon of cavity following downstream of the propeller tip in a shape resembling a corkscrew

Table 1.1: The Definitions of Different Cavitation Types as Used in CAPREX IV

1.1 Cavitation Types

While it has been accepted that different types of cavitation existed, the types have no official or clear definition. For the sake of using CAPREX IV data in modeling, the different cavitation types needed to be explicitly defined. Five types of cavitation were acknowledged in these experiments. Three of them could be defined easily: leading edge, tip vortex, and hub vortex. The last two, midchord cavitation and bubble cavitation, needed to be defined explicitly, as their distinctions were more vague and not universally agreed upon. The definitions used for each type of cavitation were as appears in table 1.1. A two-dimensional, foil experiment, discussed in appendix A, was performed, in part, to find and define midchord cavitation and bubble cavitation.

Chapter 2

Designing the Experiment

2.1 The Propeller and the Plate

The CAPREX III project had two main problems: 1) a small pressure signal from the propeller to the probes and 2) vibration induced motion on the window containing the pressure probes. For CAPREX IV, the first problem was addressed in the choice of the propeller and the distance from the outer tip of the blades to the probes. Professor Spyros Kinnas of the University of Texas at Austin chose between a small number of available propellers based on the expected pressures calculated through numerical codes. The 5 bladed surface ship propeller, a 14.63" diameter propeller provided by the David Taylor Model Basin, shown in figure 2-1, was found to have the largest pressure signal given a clearance of approximately 1.5", large enough to avoid having the tip of the propeller blades in the boundary layer of the wall containing the pressure probes.

During CAPREX III, the pressure probes were affixed to the 2" thick plexiglass window that seals the top of the test section. Since the plexiglass would bend with the same pressures that were being measured, the dynamic pressure signals were affected by the deflection of the window. To remedy this problem, the CAPREX IV pressure probes were mounted on a thick aluminum plate attached to the window. The metal plate would both decrease the amount of deflection on the wall containing the probes and be designed to the specific clearance chosen for the propeller.

To ensure that the deflections of the plexiglass window did not affect the data, the aluminum plate would be large enough to act as the top wall of the section, from the perspective of the propeller. Therefore, the aluminum plate began upstream of the window and extended the maximum allowable width of the section, making the dimensions 47" in length and 18.55" in width. Without the aluminum plate, the clearance from the propeller

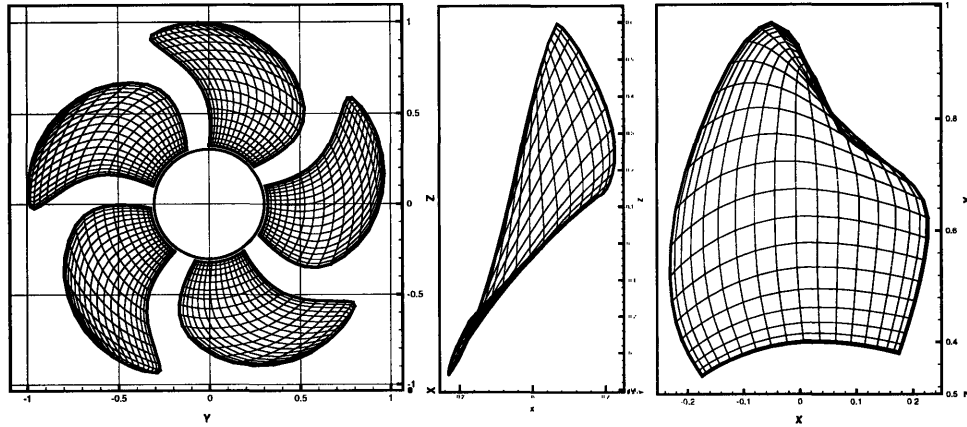


Figure 2-1: The DTMB Propeller 4842

to the tunnel window was 2.685". Since the 1.5" clearance would require a non-standard thickness to the aluminum, the decision was made to use a 1.435" clearance (approximately $0.2R$) and a standard thickness of 1.25" for the aluminum plate. The dimensions of the plate were as seen in figure 2-2.

The top side of the aluminum plate had two types of holes: through holes for the pressure probes and threaded holes for the bolts holding the plate to the tunnel window. Also on the top of the plate was a large o-ring groove for the gasket seal between the window and the plate.¹ Since no gap was needed between the window and the plate, the plate would seal to the window, which had sections cut out just above the pressure probes. The cut out sections would allow for dry access to the probes making wiring and differential port tubes easier to attach.

As mentioned above, the decision for the clearance above the propeller involved the boundary layer thickness on the aluminum plate. To decrease the affect of the plate on the inflow, the upstream edge of the plate was streamlined with a 3" long hyperbolic curve. The downstream edge was left abrupt since separation at that point would not affect the data. To create the best fit of the plate into the test section, the long sides of the plate were given a curvature matching the 3" radius, rounded corners of the test section itself. These features and the overall dimensions of the plate required machining on a large CNC

¹The o-ring was made custom by cutting a 3/8" diameter o-ring and super gluing the ring to the right length.

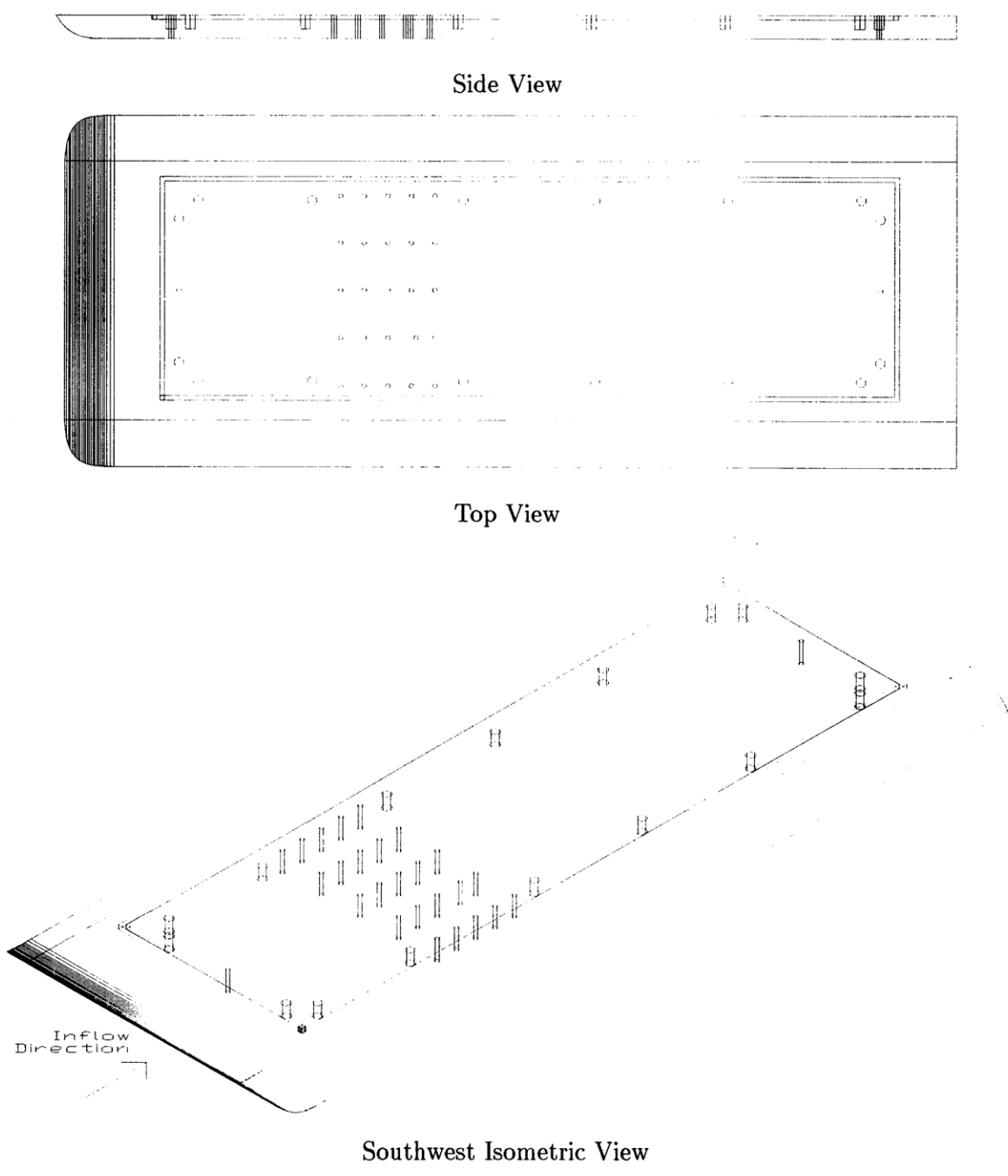


Figure 2-2: Drawing of Aluminum Experimental Plate

machine; therefore, the work was outsourced to RAMCO of Beverly, MA through the MIT Central Machine Shop.

2.1.1 The Wake Screen

To create a non-uniform flow field, an upstream wake screen was installed $18\frac{1}{8}$ " (approximately $2.5R$) before the center of the propeller hub. The non-uniformity was induced by layering metal screens so that the top of the wake screen had more layers, causing more added resistance and lower velocities. The ensuing flow field was quantified using the laser velocimetry system at the water tunnel. The coarse grid contour map of this data appears in figure 2-3. Because of the size and weight of the aluminum plate, the plate could not be rotated to acquire the other half of the plane of velocity measurements. The wake screen was symmetric; therefore, the inflow velocities were assumed to be symmetric.

2.2 The Pressure Probes

The pressure probes for this experiment needed to be inexpensive, as a minimum of 25 probes would be used. The probes had to output a voltage that could be wired into a computer data acquisition board. The computer would then be programmed to acquire the data on all channels simultaneously. Also, the probes would need to have a high frequency response and a flat response curve in the range of frequencies including the third harmonic of the propeller blade rate.

The original choice for the probe was the PX236-030GV from Omega Engineering Corporation. The probe range was 0-30 PSIG with a voltage output of 0-80 mV and a price of \$85. Because this probe read a gauge pressure, a voltage bias circuit would have to shift the zero output reading to relate to a known pressure closer to the tunnel mean pressure. This modification would allow for a tighter range of output voltages and a higher resolution on the data acquisition system (which was limited by the 12 bit hardware). Along with the voltage shift, the probe needed to be tested to find the shape of the frequency response curve.

To model the frequency response behavior, a water column affixed to a shaker would be the input frequencies for the probe, as performed in CAPREX III and seen in figure 2-4. The ratio of the pressure probe output to the output of an accelerometer affixed to the same water column should plot a flat line if the pressure probe was unaffected by the frequency of the shaker motion. CAPREX III had considerable concern about this output due to the apparent resonance in its probes. For CAPREX IV, the test was again performed

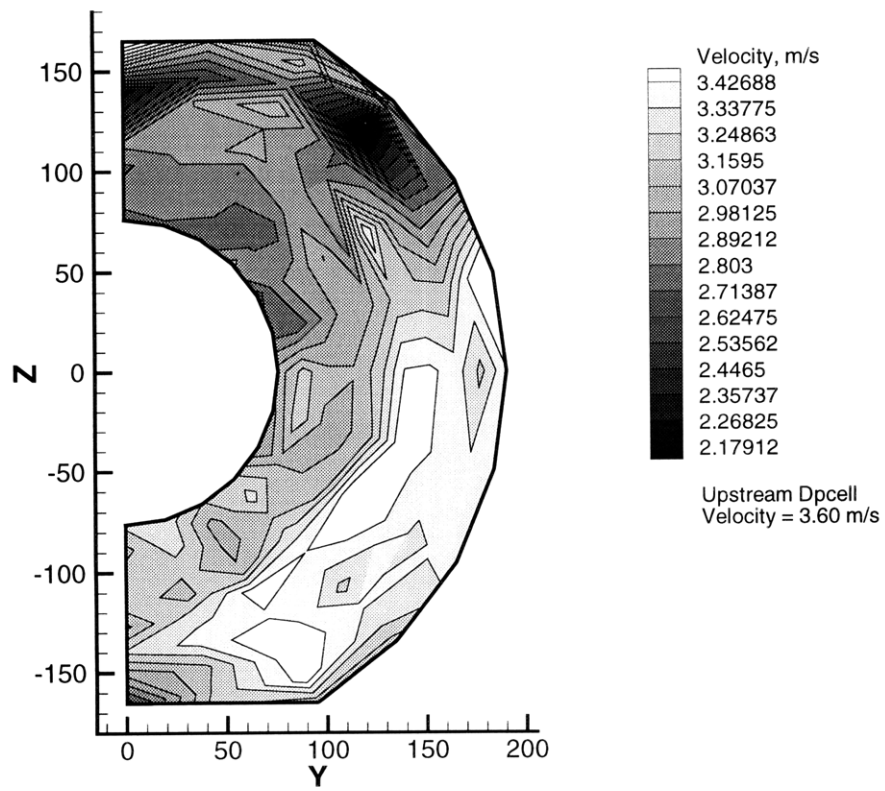


Figure 2-3: Tecplot^(R) Contour of Non-Uniform Flow Field

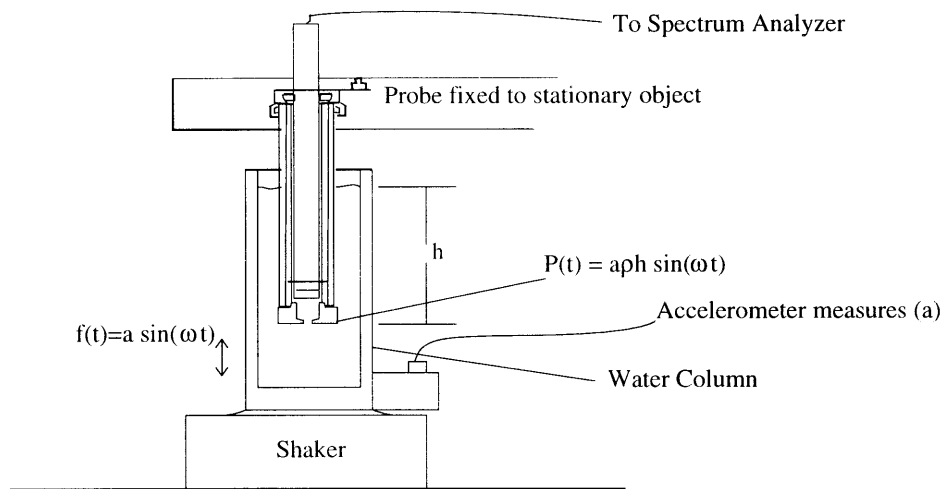


Figure 2-4: Calibration Water Column from CAPREX III Experiment

unsatisfactorily using a 100 lbf shaker from the MIT Mechanical Engineering Acoustics and Vibration Laboratory. The output plotted a curve that was more sinusoidal than flat. Since the 100 lbf shaker was not available for further tests, additional shaker tests were performed on a 1 lbf shaker borrowed from Professor J. Kim Vandiver of the MIT Department of Ocean Engineering. The Bode plots of from these test showed the same resonances as the CAPREX III tests. What was also found was that the resonance had a dependence on the height of the water in the column or the resulting hydrostatic pressure. No obvious physical resonance was found in the water column relating to the height of the water, but the assumption was made that the testing apparatus was flawed and the output from the tests should be ignored. In reference to the CAPREX III experiment, this conclusion implied that the frequency response of the probes used for that experiment might have been satisfactory, as those tests did not include different water heights for the frequency response data. Another test would need to be performed to establish the frequency response curve for those probes.

At this point in the process, the data acquisition hardware was received and a hardware limitation was found that dictated using a 0-100 mV range for the probe output into the data acquisition instead of the previously intended 0-20 mV range. The 0-20 mV range had a slower sampling rate of 60 ksamples/s versus the 200 ksamples/s of the 0-100 mV range. Since the larger range would remove a level of complexity for the circuits and the sampling rate for the experiment would have to be high, the higher range was chosen. The higher voltage range would decrease the resolution of the pressure data, so another approach to the

Propeller RPM	Output at Fundamental Frequency, mV	Output/ RPM^2
250	1.84	0.0000294
300	2.66	0.0000296
350	3.79	0.0000309
400	4.80	0.0000300

Table 2.1: Pressure Probe Calibration Test By $\frac{Pressure}{RPM^2}$ as a Constant

pressure probes was chosen. Instead, the PX26-005DV pressure probes from Omega would be used paired with one PX26-030GV probe. The PX26-005DV probes are differential pressure probes with a 5 mV of output per 5 V excitation over a 0-5 PSID differential pressure range and a cost of only \$32. The increased resolution of the differential probes was attained by linking the probes to the mean pressure of the tunnel through an external bladder. A 0-30 PSIG, PX26-030GV probe would then record the tunnel mean pressure so the total pressure at every sample could be found through simple algebra.

The frequency response test for the PX26 series probes was performed in the tunnel using the propeller directly. A single probe placed above the center of the propeller hub on the aluminum plate was wired into an oscilloscope which was also reading a propeller rpm trigger. The relationship between the pressure and the square of the propeller rotation should be constant for a constant advance coefficient. The ratio of the pressure probe output at the primary harmonic divided by the trigger reading of the propeller rpm squared should also be constant, if the probe was unaffected by the propeller frequency. For four different rpm between 250 and 400 and a constant advance coefficient at design value of 0.91, the relationship was found to be constant within a small error value (as seen in table 2.1), and the probes were deemed to have a sufficiently flat response curve.

2.2.1 Excitation Voltage and Wiring

The maximum excitation voltage for the PX26 series pressure probes was 16 VDC, with a recommended 10 VDC and a 0-50 mV output. Since the output range was dependent on the excitation voltage, all of the probes should be powered from the same reliable source. Since a 60 Hz frequency often accompanied the signal from a voltage source unit, a 12 V car battery was chosen for the excitation voltage, specifically an ACDelco Profession Freedom Car and Truck Battery model 26-5YR.

The PX26 series pressure gauges have four electrical pins: high and low excitation voltage and high and low output signal. Omega Engineering recommends their CX136-4 as the mating connectors for the PX26 probes. To connect the probes to the excitation voltage and the data acquisition hardware, equal lengths of DigiKey two pair, shielded, multiconductor cable (part number A131-100-ND) were soldered to the CX136-4 connectors at one end and separated into groupings at the other. The wires were soldered in order by common color denominations to help in identification: red wires to positive excitation voltage, black to negative excitation voltage, white to high output signal, and green to low output signal. The three wire groupings included high and low excitation voltage groups soldered around wire terminals and a third group that connected into the screw-terminal panel for the data acquisition.

2.2.2 The Differential Pressure Bladder

In order for the output from the differential probes to be easily transformed into gauge pressure values, all of the differential vent ports were tied to a single known pressure. Using lengths of $\frac{1}{8}$ " inner diameter, vinyl tubing, each probe was connected to a large, enclosed PVC bladder which was then tied to tunnel mean pressure through a tunnel reference. One differential probe and the gauge probe separately recorded the pressures from the bladder creating a simple algebraic equation to transform the differential pressure output into gauge pressure values.

The PVC bladder was constructed from a 2' long, 6" diameter pipe with end caps sealed over both ends. The connection to tunnel mean pressure was through a single hole in the center of one of the end caps while the differential probes connected to holes in two rows along one side of the pipe length.

2.3 Data Acquisition System

2.3.1 Hardware

To be able to see the pressure changes above the propeller, the data had to resolve the frequency at which the blades pass the probes to the third harmonic. For this, the probes would have to sample a minimum of 12 points within the period of the third harmonic. Since the rotational speed of the propeller for the exact tests was unknown and a new, untested dynamometer was on the propeller shaft, a 1200 rpm maximum allowed rotation for this propeller on the shaft was used to calculate the data sampling rate. The data rate

was calculated from the equation

$$1200 \text{ rpm} \cdot \frac{1}{60} \cdot 3 \text{ harmonics} \cdot 5 \text{ blades} \cdot 12 \text{ points} = 3600 \frac{\text{samples}}{\text{second}}. \quad (2.1)$$

Such a high sampling rate would be a limitation on the choice for the data acquisition hardware. The other limitation was the number of data channels to be sampled. The differential probes would include a 5×5 array above the propeller to take the bulk of the data. Also, a probe upstream and one downstream would act as reference points for the computer modeling. The next two probes would measure the link from the differential probes to the mean tunnel pressure. Lastly, one channel would capture the rotation of the propeller from an electronic trigger and one channel would track the excitation voltage from the battery. The total channel count was 31.

The Keithley-Metrabyte DAS-1800 HC series data acquisition board was the only board found that dealt with both of the limitations. The board series could take 32 differential inputs with an advertised maximum sampling rate of 312.5 ksamples/second. Particularly, the DAS-1801 HC board could handle the bipolar input range ± 100 mV with a maximum sampling rate of 200 ksamples/second. Unfortunately, the board could only use two DMA channels on the computer limiting the capacity to 131,072 points when bypassing the CPU for faster data acquisition. The associated accessories to the board included a STP-100, 100 pin screw terminal panel and a 10' CAB-1803, 100 pin cable.

2.3.2 Software

On recommendation from Keithley-Metrabyte, the TestPointTM software from Capital Equipment Corporation was purchased with the DAS-1801 HC board to create data acquisition programs. TestPointTM was recommended because of its simple, visual interface and compatibility with Keithley products. TestPointTM was used to create two basic applications: a calibration program which wrote a calibration file of averaged probe voltages for a set of hydrostatic pressures and an experimentation program which acquired the data from all of the channels at a given sampling rate and output a data file as well as a Fast Fourier Transform (FFT) and time series plots drawn on screen for any chosen channel.

The Calibration Program

The simplest way to calibrate all of the pressure probes would be to use the height of the water in the tunnel to change the hydrostatic pressure seen by all of the probes simultaneously. A TestPointTM application was written which would double as a calibration program

and a method to check the probe channels by displaying an average of samples on the screen. The program had two pushbutton objects². The first pushbutton would sample all of the pressure probe channels and average the output. The averaged values would then appear on screen in display objects³ labeled with the channel numbers as defined for the DAS-1801 HC board. The second pushbutton would output the averaged values and an input height value as a column in a tab separated, text file called `calibration.dat`. The file would then be used with a Matlab^(R).m file (see appendix B) to calculate the least squares fit regression for the probe voltage output versus pressure measured in pascals.

The Experimentation Program

Since some of the most interesting cavitation was both loud and possibly destructive to both the water tunnel and the propeller, the experimental program had to be simple to use quickly. For the same reasons, a valuable feature of the program would be to plot some of the data immediately as a check that everything was working properly. *Experiment*, a TestPointTM application, was written to cover both of these bases and more. *Experiment* performed three separate actions: taking the data, outputting the data to a specified file, and graphing the FFT and time series for any single channel with or without a low-pass filter. Each of the mentioned actions had its own pushbutton.

The main section of the application acquired the data. Allowing for flexibility in the experiment, the sampling rate and the channels to be sampled were both modifiable variables. The initial values of which were a data rate of 3600 Hz and channels 0 through 30 (the values used for this experiment). By using the TestPointTM container objects⁴ the hardware limitation on sampling was circumvented. The application was hardwired to take 20,000 samples at the input data rate of the input channels. The increased number of data points (620,000 total points for the initial value settings) was achieved by putting the data from every 4,000 samples into one of five containers. The final data set was then the compilation all five of the containers. Also hardwired into the application was a gain setting for the data acquisition board for acquiring ± 100 mV data.

The second section of the application could view the most recent data set. By inputting a channel number into the Channel to graph data-entry object⁵ and clicking on the Graph pushbutton, the user could graph the FFT for all of the samples on that channel and a times

²Pushbutton objects were Windows style buttons which could be clicked by the user to trigger an action list[4]

³Display objects showed strings or numeric data in a selected size, color and format[4]

⁴Container objects provided temporary storage of data and the ability to accumulate data [4]

⁵Data-Entry objects provided for user input of variable values, either numeric or strings [4]

series graph of the first 360 samples to the screen. Using the Filter Data switch object⁶ before clicking Graph, the user could choose to perform a low-pass filter with a 500 Hz cut off frequency before graphing the channel data.

The last section of the application wrote the data to a file. After inputting the full path name of the desired output file to the Filename data-entry object, the entire data set could be output by clicking on the Output to File pushbutton. The initial value of Filename was set to the path of a specified CAPREX directory to keep all of the files together on the computer.

⁶Switch objects let the user choose between an on or off setting for a variable[4]

Chapter 3

Performing the Experiment

3.1 Installing the Plate

Installing the aluminum plate into the Water Tunnel did involve a little maneuvering. The openings in the test section were 43" long by 13.5" tall with a 20" internal width to the tunnel itself. The aluminum plate's dimensions were 47" long by 18.55" wide by 1.25" thick, and the plate was heavy. The method used to get the plate attached to the top window of the test section was as listed in table 3.1. The installation involved three people, but could probably be done with only two.

3.2 Installing the Pressure Probes

Setting up the pressure probes was more frustrating than complicated. To seal the probes to the plate, a washer with an o-ring as its inner diameter went over the wet port of each probe. For each column of probes, a strip of aluminum was drilled with through holes for the probes and staggered holes for small bolts which screwed into the plate, putting pressure down on the probes to seal the o-ring washers, as shown in fig 3-1.

The probes were numbered 0 to 28, ordered upstream to downstream, west to east (as oriented in place on the water tunnel) as shown in figure 3-2. For book keeping, the probe numbers were the same as the respective channel numbers for the data acquisition system. The channel numbers were written on the CX136-4 connectors wired into the STP-100 terminal panel. The STP-100 panel was separated into two sections which related to the two sides of the 100 pin connector to the DAS-1801 HC board. The sections were marked A and B, with B being the side closest to the cable connection. The pin diagram for the STP-100 and DAS-1801 HC was as in figure 3-3[6]. The remaining two channels were wired

1. With both side windows removed from the section and the upper and lower windows in place, lift the plate into the test section perpendicular to the normal position. Be sure that the top of the window is directed up and the o-ring is in place.
2. Holding the plate at both ends, rotate the plate so the upstream end of the plate is at the top, upstream corner of the side opening and the downstream end is at the bottom, downstream corner of the other side opening.
3. Being careful of the corners, continue this rotation until the plate is in the correct orientation inside the test section.
4. To lift the plate up to the top window, slowly step the plate higher by stacking blocks of wood under the plate. Alternate at the upstream and downstream ends. This allows the plate to be lifted without ever requiring more than a few inches at a time.
5. Once the plate is lifted to within one half to one quarter of an inch from the top window, shift the plate in its plane to line up the bolt holes. A person on top of the tunnel to watch and direct the movement will make this go faster.
6. When at least two holes are lined up, finish bolting the remaining 14 bolts. Be careful not to bolt down so tight as to damage the plexiglass window or the bolt threads. The gap between the window and the plate will not be completely closed because of the thickness of the o-ring.

Table 3.1: Steps to Install the Aluminum Plate

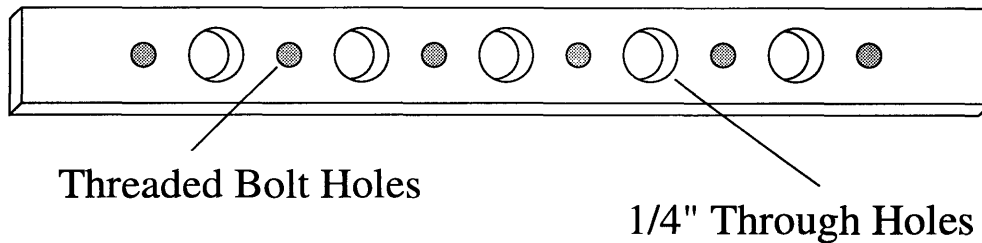


Figure 3-1: Aluminum Strips for Arranging and Holding Pressure Probes onto the Experimental Plate

⑳ Bladder Differential Probe

㉑ Tunnel Mean Gauge Probe

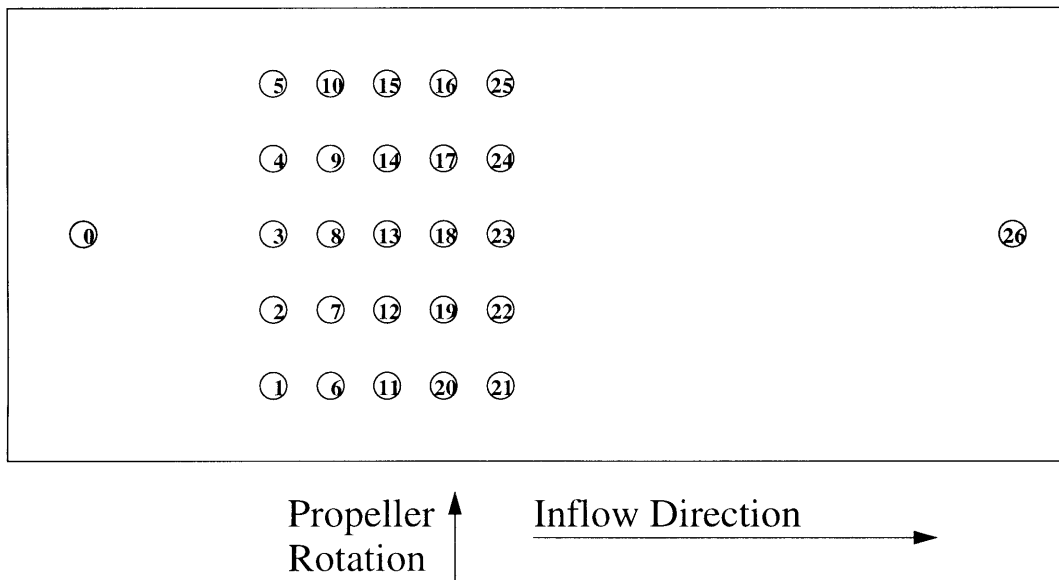


Figure 3-2: Numbering Scheme for Pressure Probes

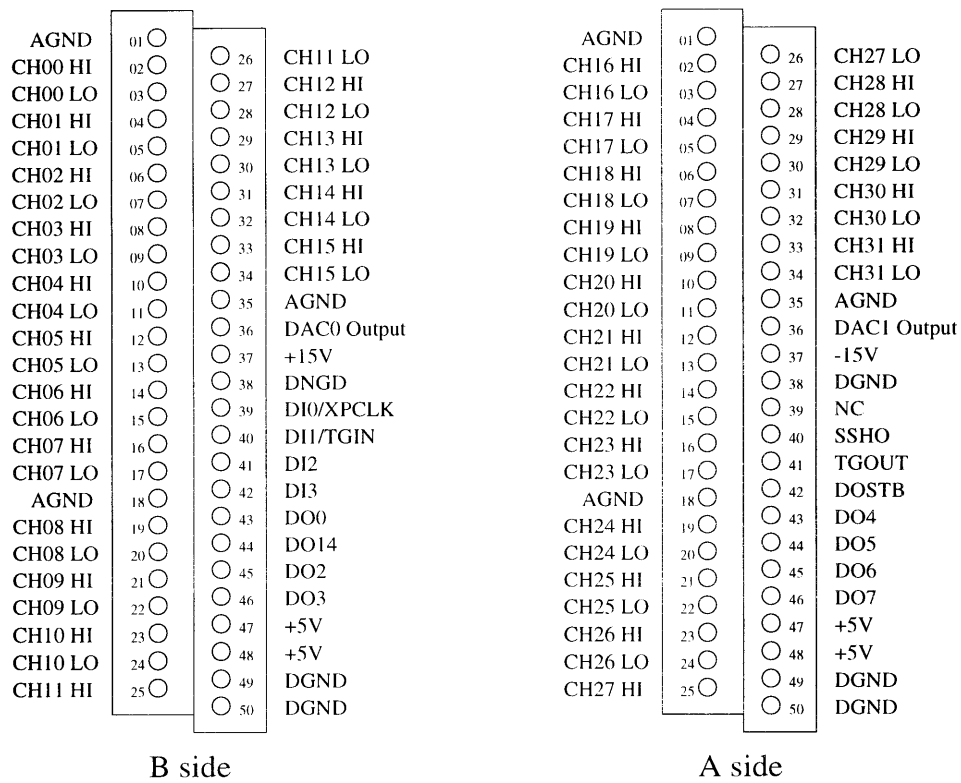


Figure 3-3: Pin Diagram for STP-100 and DAS-1801 HC

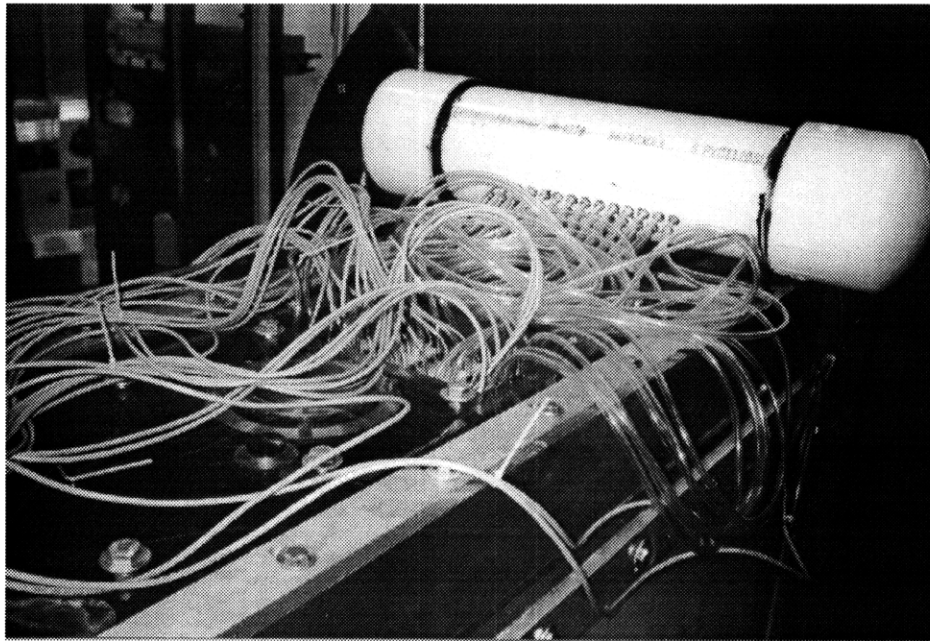


Figure 3-4: Photograph of PVC Bladder Setup and Location

into the the STP-100 panel via a bread board containing voltage dividers which translated the trigger and battery signals into the ± 100 mV range.

Each pressure probe was then connected by vinyl tubing to a hose connector on the PVC bladder. The bladder sat on top of the tunnel at the upstream end of the test section with the two lines of hose connectors facing directly downstream, as seen in the photograph in figure 3-4. The end cap, hose connector was then connected to a reference point on the tunnel above the test section. The last differential probe, channel 27, was connected between the PVC bladder and a tube to tunnel mean pressure. Also connected to tunnel mean pressure was the gauge probe, channel 28.

3.3 Running the Calibration Program

The TestPointTM calibration program was called *ChannelCheck*. *ChannelCheck* created a *calibration.dat* file of averaged values for each pressure probe channel at an inputted height of water in the tunnel. This data file could then be used to calculate the calibration constants which transformed the mV outputs into pascal pressures. A variant on *ChannelCheck*, *Zeros* could read the output from all 31 data channels simultaneously and show the averaged

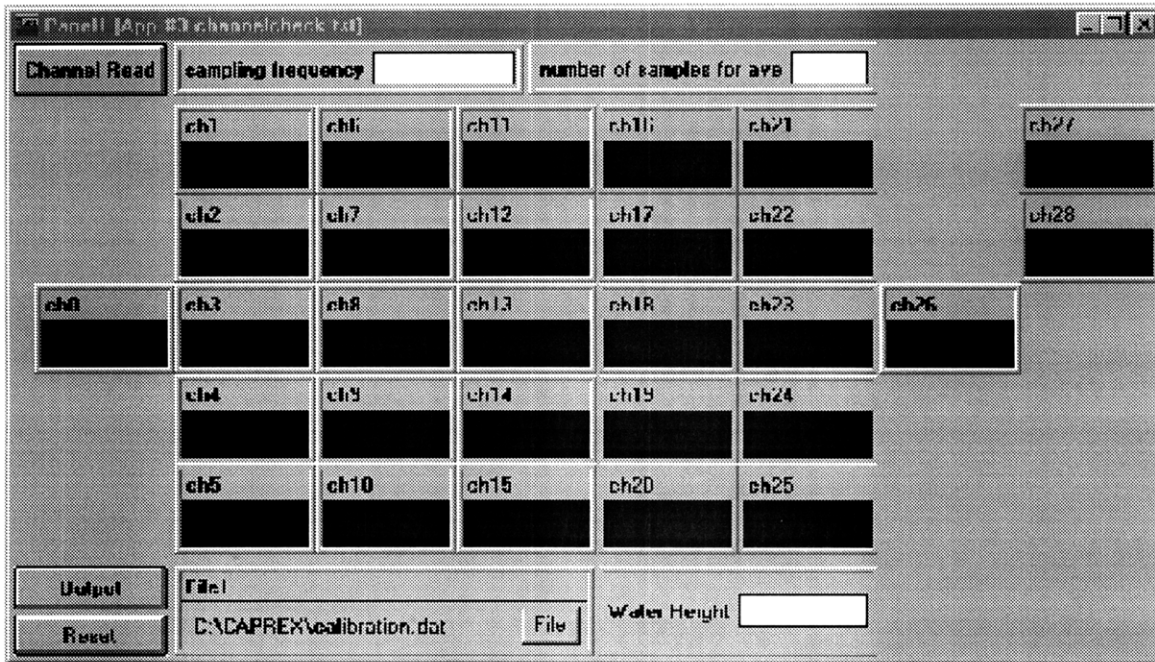


Figure 3-5: On-screen Panel View of the *ChannelCheck* application

values for each channel on screen. By looking at *ChannelCheck* or *Zeros*, overloads and far off values could be detected before running the experiment.

ChannelCheck was designed to visually represent the probes with its on-screen display, as seen in the panel screen view of *ChannelCheck* figure 3-5. The Channel Read pushbutton in the upper left corner of the panel activated the sampling. At the top of the panel screen, both sampling frequency and number of samples for ave[range] appeared in data-entry objects that could be changed for faster sampling rates or more samples used toward each average. The initial values for each were 100 Hz and 10 samples. In the center of the panel were all of the channel output display objects which reported, onto the screen, the averaged values. The arrangement of the channel display objects was specifically chosen to resemble the top view of the experimental plate, making obvious the connection between a bad value on the screen and a specific probe in the apparatus. At the bottom right of the view, was a data-entry object for the water height in the tunnel. Using a ruler attached to the tunnel's water level view glass, relative heights were measured in centimeters and their numerical values were input to this data-entry object. The input height was saved in *calibration.dat* as the first column of information. At bottom left were two additional pushbutton objects,

1. Run the application from Start Menu/Programs/TestPoint/ChannelCheck.
2. A window will appear while the program identifies the DAS-1801 HC data acquisition board, if an error window appears afterward check that the board has been properly plugged into the computer and setup within the system (see DAS-1800 HC series manual for proper initialization and/or TestPointTM help window on the setting up A/D boards for autofind).
3. Change the sampling frequency and number of samples for ave[range] as needed by clicking on the data-entry objects and typing in new values.
4. Enter in the relative height of the water in the tunnel view glass into the Water Height data-entry object.
5. Click on the Channel Read pushbutton.
6. Modify the water height in the tunnel and repeat the last two steps for as many different hydrostatic pressures as desired.
7. Click on the Output pushbutton to write the list of heights and channel outputs to the filename at the bottom of the panel screen.
8. If you would like to just check the channel values before performing the calibration, use the Channel Read pushbutton to display channel output values and then click on the Reset pushbutton before running the actual calibration.

Reminder: If you click on the Reset pushbutton during the calibration, all of the previous data will be erased and you will need to start the calibration over.

Table 3.2: Steps for Running the Calibration Application

Output and Reset. Each time that the Channel Read pushbutton was clicked, the water height and channel average values were written to a list¹. Channel Read could be used to view the values of pressure probe channels alone. Before doing the calibration, Reset had to be clicked to empty the existing list from memory. Once the calibration was complete, the Output pushbutton wrote the list of heights and associated outputs to a file. The file was initially set as *C:\CAPREX\calibration.dat*, but could be changed by clicking the File button and choosing another output file. Step-by-step instructions on running the *ChannelCheck* application could be found in table 3.2

3.4 Running the Experiment

The *Experiment* TestPointTM application performed three actions: sampling the data, graphing sections of the data to the screen, and writing the data to a file. Each of these actions

¹ A list was a data type made up of any number of other data types, in this instance of vectors/citeTPT

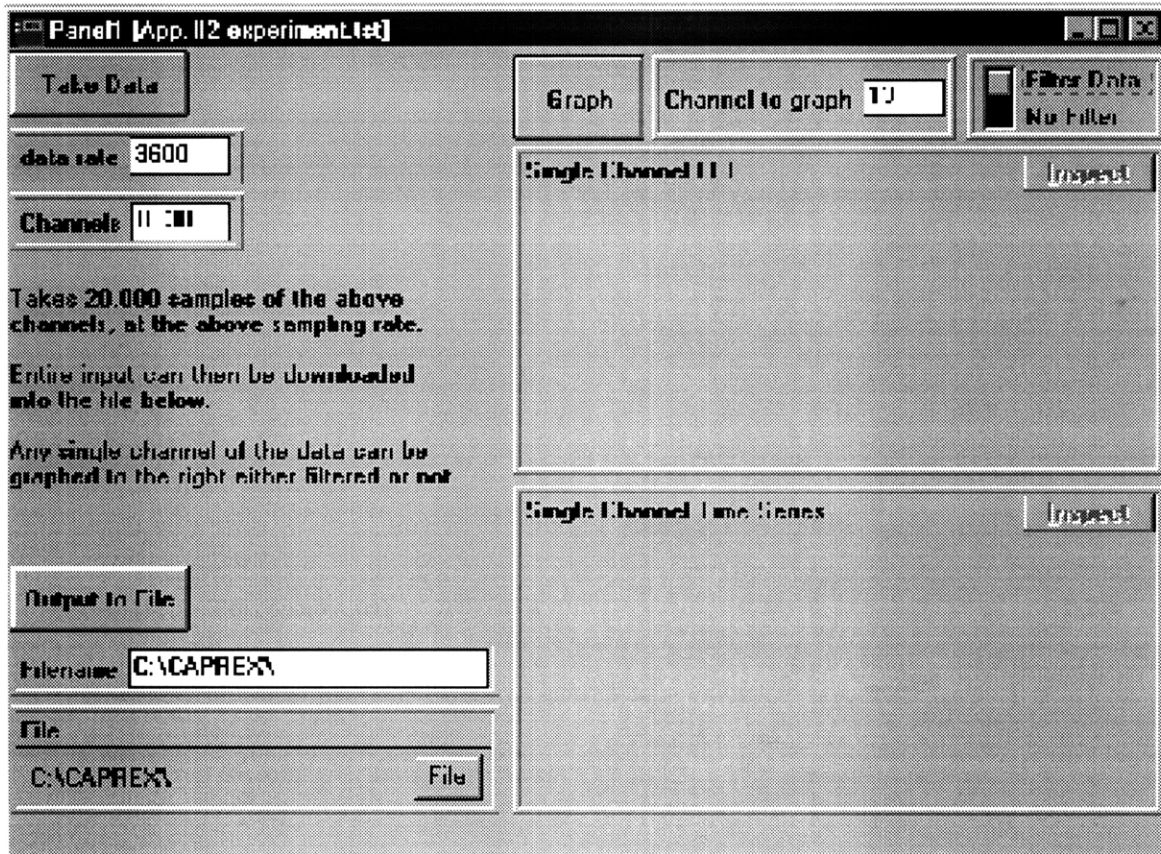


Figure 3-6: On-Screen Panel View of the *Experiment* Application

were found in an area of the screen with any data-entry or switch objects associated with that action, as seen in figure 3-6.

3.4.1 Take Data

The upper right hand corner of the *Experiment* panel screen contained the three objects involved with acquiring the data for the experiment. Every run of the experiment would take 20,000 samples of data, but the sampling rate and the channels to be sampled could be adjusted. The data rate data-entry object had an initial setting of 3600 Hz, but could be modified for different rates. The DAS-1801 HC board had a 312.5 ksamples/second which included all of the samples on all of the channels read, no data rate should be input that exceeds this limit. The Channels data-entry object had an initial setting of “0..30” which told the program to sample from all channels starting at 0 and ending at 30. Single

channels could be removed by listing all of the channel numbers separated by commas as with “0,2,3,4”, or by having multiple groupings separated by commas “1..15,27..30”. To take the 20,000 samples for the data rate and channels entered, the Take Data pushbutton was clicked.

3.4.2 Graph

With data files of approximately 9 MB, viewing the data before creating the output file could save time and trouble, ferreting out possible problems during testing. For this reason, the second part of the *Experiment* application visualized any channel of data, for the most recent data set, on two graphs. The Channel to graph data-entry object had an initial value of 13, the channel in the center of the 5×5 pressure probe array, but could be changed to view other channels. At the very top right of the panel screen was a Filter Data/No Filter switch object which could be switched to Filter Data by clicking the black space next to the choice (the gray square would be next to whichever was the present choice). If the Filter Data switch was on (Filter Data chosen), the graphs would show the channel data after being recalculated with a low-pass filter of a 500 Hz cut off frequency. The Graph pushbutton calculated the Fast Fourier Transform for the entire run of data on the channel selected and then graphed the FFT on the top graph and a time series for the first 360 data points on that channel on the lower graph. When the graphs were on screen, the Inspect button could be used to create a larger, single window containing the graph. This pushbutton could be used for additional channel settings for the last data set taken.

3.4.3 Output to File

Once the data had been taken, whether graphed or not, it could be output to a file. The Filename data-entry object had an initial value of the C:\CAPREX directory, but a file name must be input for each experimental run. The File at the bottom left corner of the panel screen showed the last file name used, but otherwise need not be touched. When ready to write the data to a file and the file name had been entered, the Output to File pushbutton would be clicked. Step-by-step instructions in how to use the *Experiment* application, could be found in table 3.3.

1. Run the application from Start Menu/Programs/TestPoint/Experiment
2. A window will appear while the program identifies the DAS-1801 HC data acquisition board, if an error window appears afterward check that the board has been properly plugged into the computer and setup within the system (see DAS-1800 HC series manual for proper initialization and/or TestPointTM help window on the setting up A/D boards for autofind).
3. Change the data rate or channels to be sampled as needed by clicking on the data-entry objects and typing in new values.
4. Click on the Take Data pushbutton; it will appear to be pushed in (notice the shaded edges). When data is finished sampling, the Take Data pushbutton will appear to be “out” again. Be sure to wait the few seconds this takes.
5. Set Channel to graph by clicking on the data-entry object and typing in the new value, and choose whether or not to filter the data by clicking on the space next to your option (the choice with the gray square next to it is on).
6. Click on the Graph pushbutton.
7. If you would like to see additional channels, or want to change the filtering choice repeat the last two steps as many times as you want.
8. Name the output file by clicking on the Filename data-entry object and typing in the appropriate file name.
9. Click on the Output to File pushbutton.
10. Repeat the entire process for each different set of propeller parameters. You will see that not all of the steps are required, do the ones you want.

Note: Since the output files are so large, your PC may not want too many files on its hard drive at a time. If this is true, ftp the file to another machine and erase old files as you go. After a lot of runs, the PC may act up; try restarting *Experiment* or if necessary the entire computer.

Table 3.3: Steps for Running the *Experiment* Application

3.5 Processing Data

Once the data sets were transferred to a local UNIX machine, two programs were used to process the information. The first program was written as a Matlab^(R).m file, and it created a file of calibration constants from the data found in *calibration.dat*. The second program was a Fortran program which used the calibration constants to transform the data into engineering units, in this case pascals, and wrote an ASCII Tecplot^(R) file which could be animated to see the pressure changes above the propeller over time.

The calibration program, in appendix B.1, read in the *calibration.dat* file and performed a least squares, linear, regression to find the calibration constants for each individual pressure probe. The value of atmospheric pressure (in mmHg), on line 7 of the program, should be changed to be the barometric reading when the experiment was run. The program treated the last channel in the *calibration.dat* file as the gauge probe. The constants were then written to a file called *calibconstants.dat*.

The Fortran program, in appendix B.2, asked the user for an input data file and then used the *calibconstants.dat* file to translate the raw voltage data into calibrated pascal units. Next, the programs asked the user for a Tecplot^(R) file name to which it wrote an ASCII Tecplot^(R) data file of three variables: location in stream wise direction (X), location across the tunnel (Y), and data output value in pascals (OUTPUT). The locations were defined in inches with the origin at channel 13, the probe in the center of the array, and the values increasing going downstream and moving away from the viewing window (in the same direction as the probe numbers increased). For brevity, the program only output the first 1600 samples of the 5×5 array of pressure probes above the propeller. Slight modifications to the program could change the number of samples output while somewhat more complicated modifications could add the upstream and downstream probes to the Tecplot^(R) file.

To see the output, the ASCII Tecplot^(R) data file was opened in Tecplot^(R) as a contour plot on the OUTPUT variable with contour levels auto set by the program. The first sample of output would appear in a rectangular contour plot on the screen. By animating the plot on values of K, the time steps for the pressure data would appear as a movie on the screen.

Chapter 4

Experimental Results

4.1 Cavitation Conditions

The intention of this experiment was to capture both tip vortex and midchord cavitation as pressure values in a plane above the propeller. Unfortunately, the 4842 propeller had never been run in the MIT water tunnel to find out what types of cavitation happened at which conditions. Also, time constraints meant that the data would have to be taken at the same time that the cavitation was initially observed, without knowing what would happen when. The photographs in figures 4-1 through 4-12 showed the cavitation captured in each experimental run. For identification, each run was tagged with a letter, due to some problems during experimentation, some lettered runs were omitted from the set of 12 experimental runs. Luckily, the runs performed included the tip vortex type cavitation in a variety of strengths and sizes, in figures 4-1 through 4-11, and the midchord bubble cavitation was captured in two different runs, in figures 4-8 and 4-9. Also, at least three runs included leading edge cavities, figures 4-3 through 4-5.

The differences in cavitation behavior for each experimental run related to the advance ratio J and the cavitation coefficient σ defined by [11] in equations 4.1 and 4.2 respectively:

$$J = \frac{U_\infty}{nd} \quad (4.1)$$

where U_∞ was the upstream Dpcell velocity, n the rotational speed of the propeller per second, and d the diameter of the propeller, and

$$\sigma = \frac{p_o - p_v}{\frac{1}{2}\rho U^2} \quad (4.2)$$

where p_o was the ambient pressure of the flow, p_v the vapor pressure of the fluid, and ρ the density of the fluid. The advance ratios and cavitation number for each experimental run

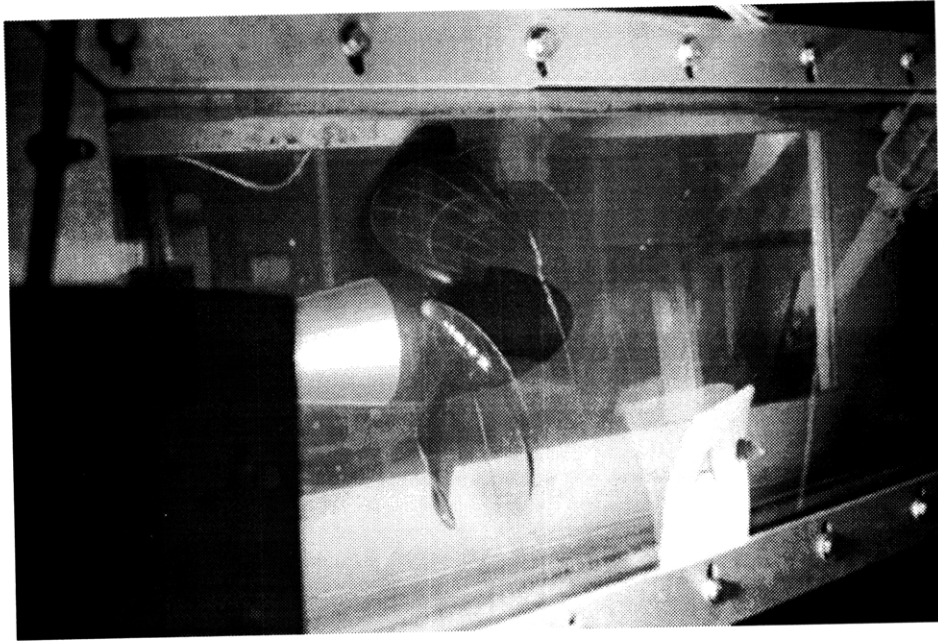


Figure 4-1: Photograph of Experimental Run A



Figure 4-2: Photograph of Experimental Run B

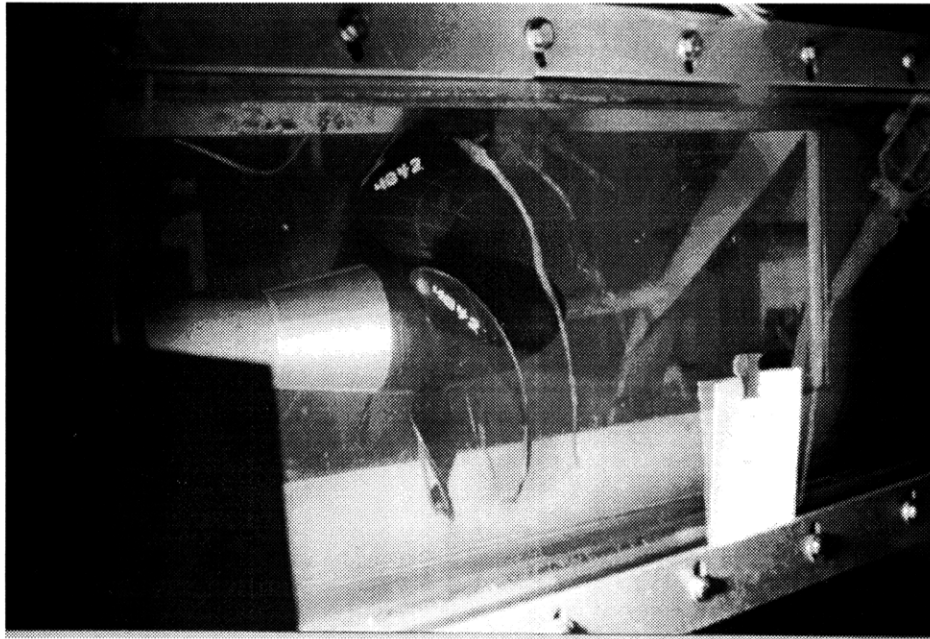


Figure 4-3: Photograph of Experimental Run C

were listed in table 4.1.

4.2 Dynamic Pressure Output

The data acquired through the pressure probes was visualized through contour graphs of the pressures animated over a time. For the purposes of this document, multiple frames of these animations have been compiled into figures 4-13 through 4-24. Using the data from channel 30, the propeller rpm trigger to identify the relative location of the propeller for a given sample, the sequence of frames in these figures covered $\frac{1}{5}$ of a revolution, or one blade passage. The pressure changes as the blade passed the probes could be seen in the animations: a high pressure preceded the blade, and then a low pressure followed it. The slight angle in the positive X, positive Y direction agreed with the movement of the wake downstream along the skew angle of the propeller.

The accuracy of the pressure probes had been a major concern during the experiment, especially after issues raised about the probes used in the CAPREX III experiment. One method by which the dynamic pressure could be checked was by looking at the FFT of the entire data set for a single channel. Because of this, the experimental program displayed

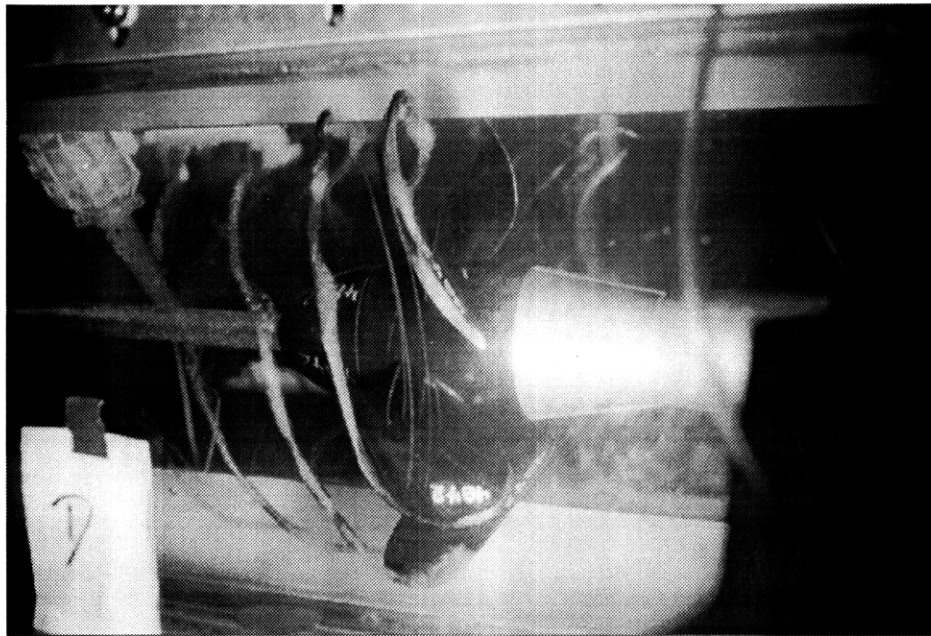
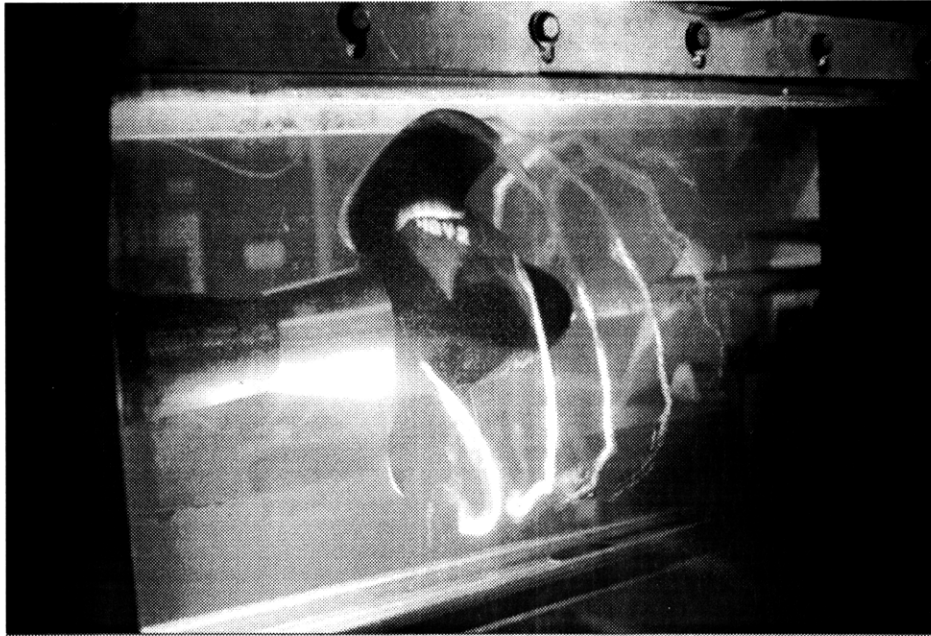


Figure 4-4: Photographs of Experimental Run D from Both Sides of the Test Section

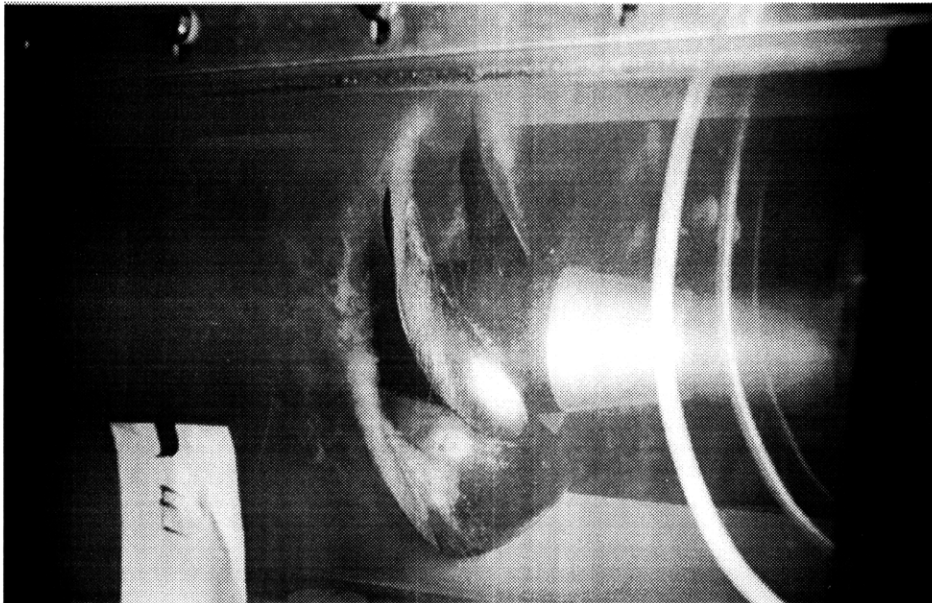
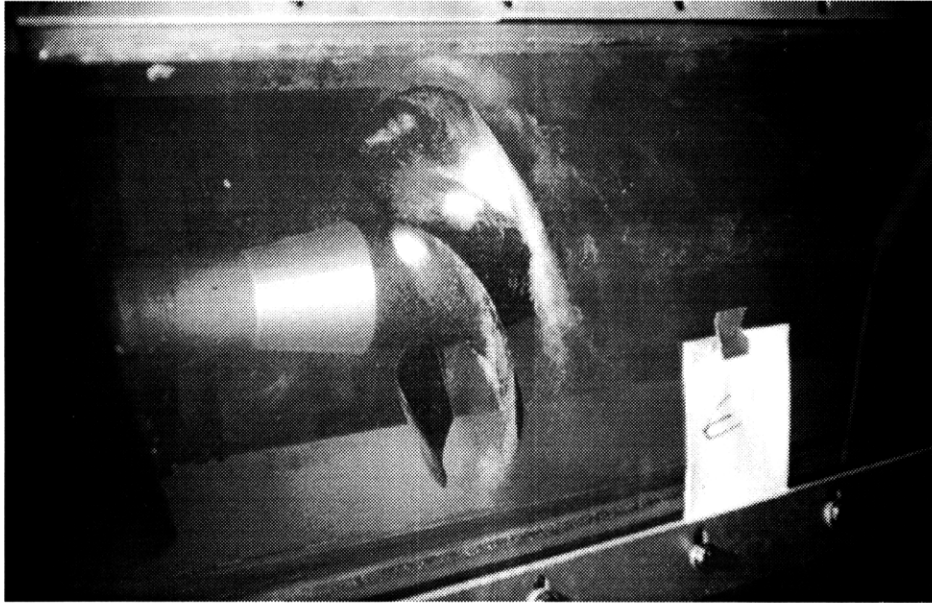


Figure 4-5: Photographs of Experimental Run E from Both Sides of the Test Section

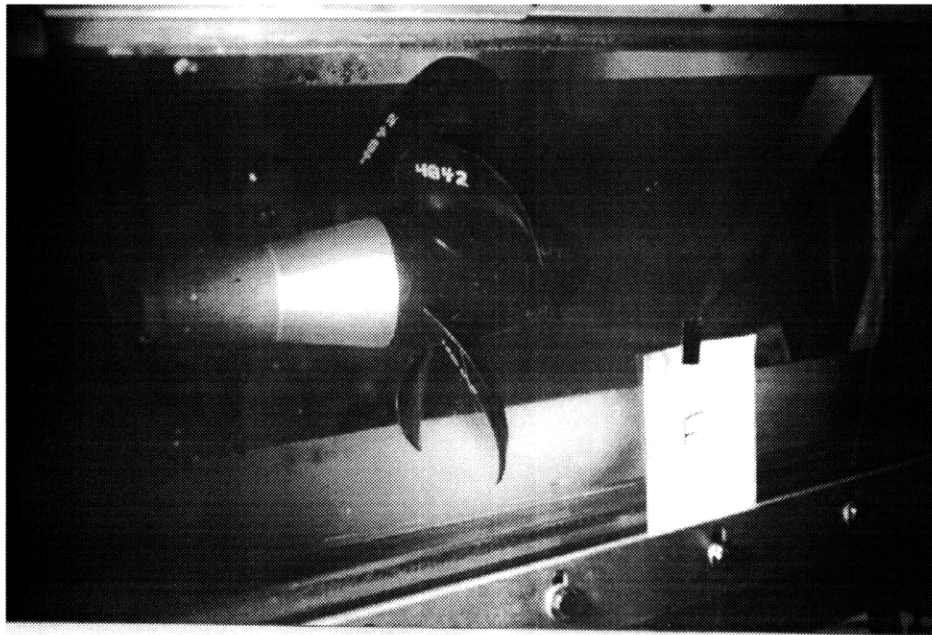


Figure 4-6: Photograph of Experimental Run F

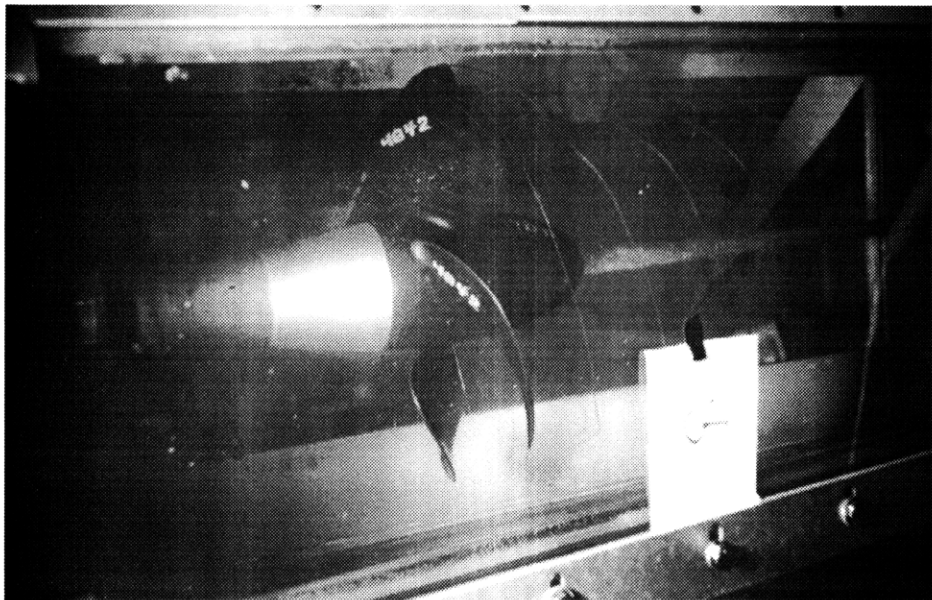


Figure 4-7: Photograph of Experimental Run G

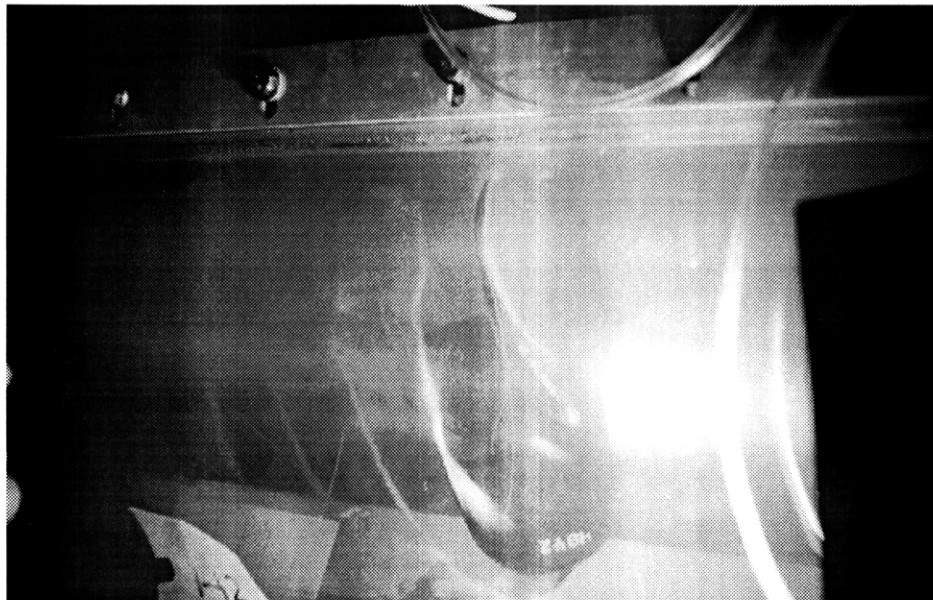
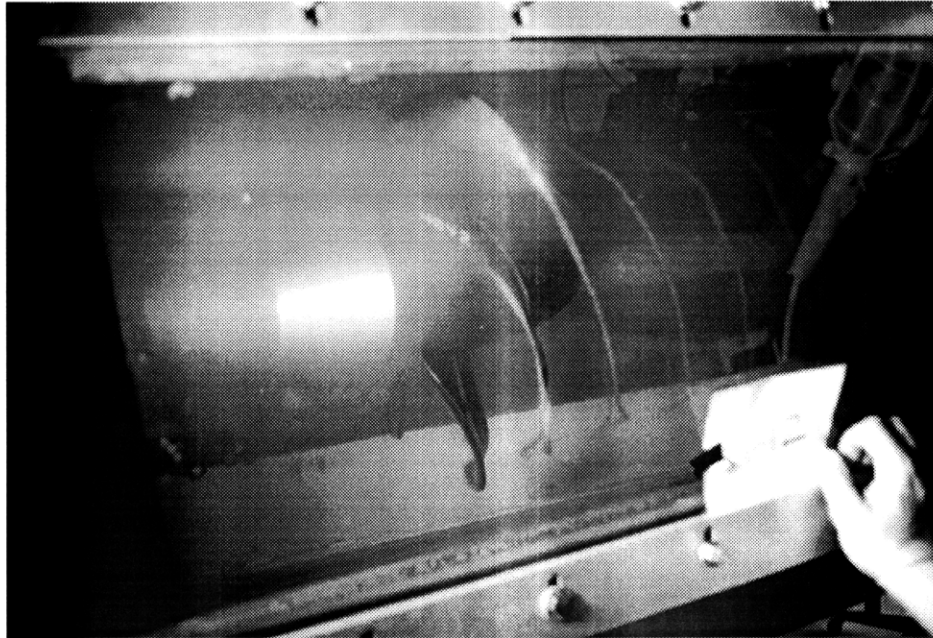


Figure 4-8: Photographs of Experimental Run H from Both Sides of the Test Section

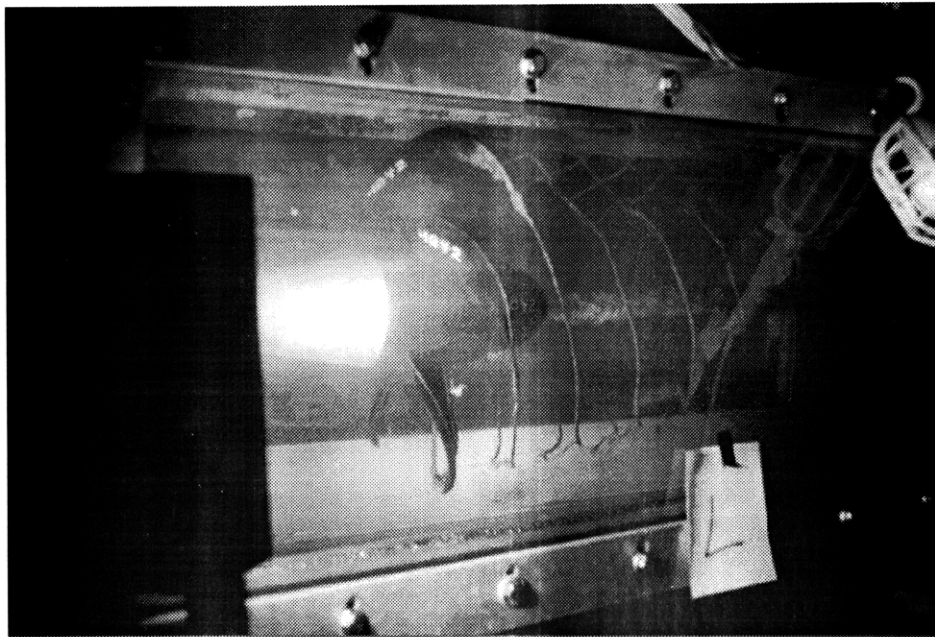


Figure 4-9: Photograph of Experimental Run L

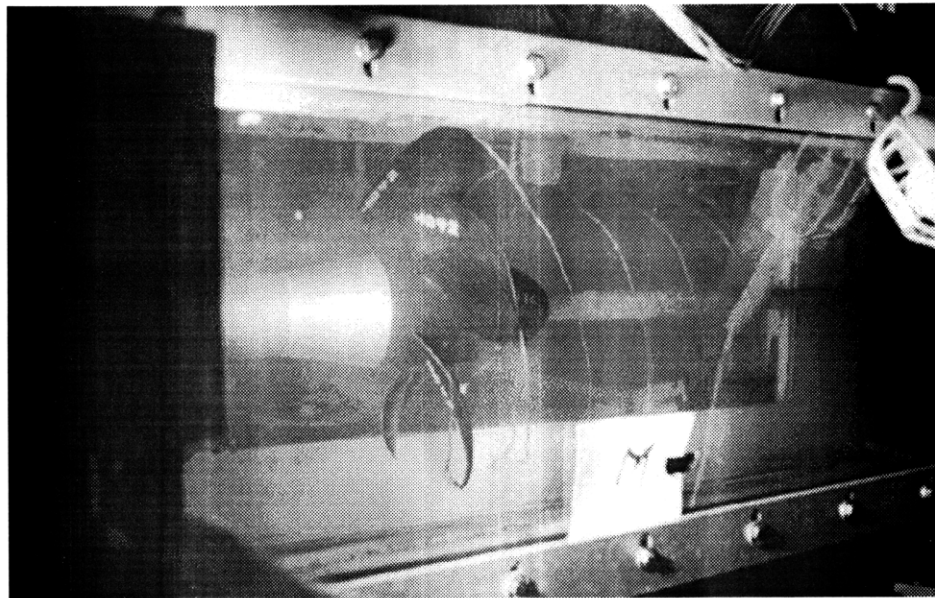


Figure 4-10: Photograph of Experimental Run M

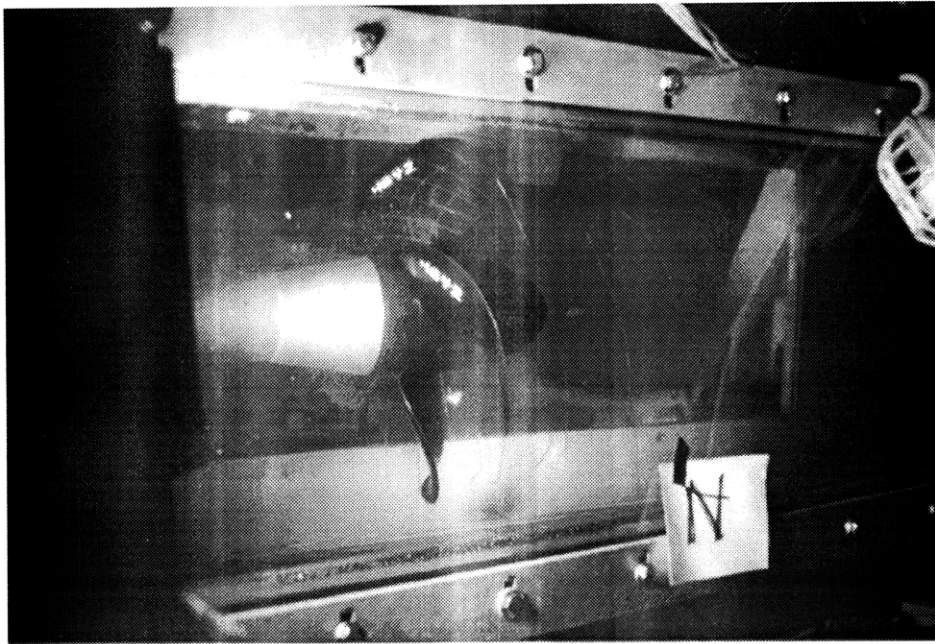


Figure 4-11: Photograph of Experimental Run N

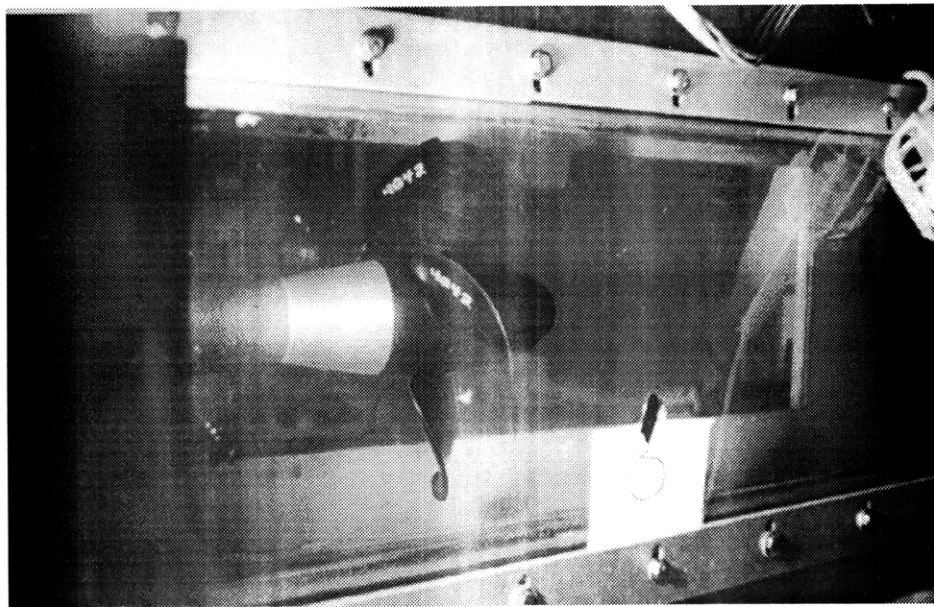


Figure 4-12: Photograph of Experimental Run O

Run	Impeller Speed $\frac{ft}{s}$	Propeller Speed rpm	Tunnel Pressure kPa	J	σ
A	8.62	707	65.2	0.60	17.89
B	8.60	708	51.3	0.60	13.92
C	8.56	704	46.3	0.60	12.58
D	8.62	706	41.2	0.60	10.91
E	8.20	705	35.1	0.57	10.11
F	11.66	700	65.3	0.82	9.80
G	11.66	700	51.3	0.82	7.57
H	11.38	695	35.8	0.81	5.36
L	11.85	685	36.7	0.85	5.09
M	11.82	683	39.2	0.85	5.50
N	11.84	683	50.2	0.85	7.17
O	11.82	682	65.6	0.85	9.58

Table 4.1: Advance Ratio and Cavitation Number for Each Experimental Run

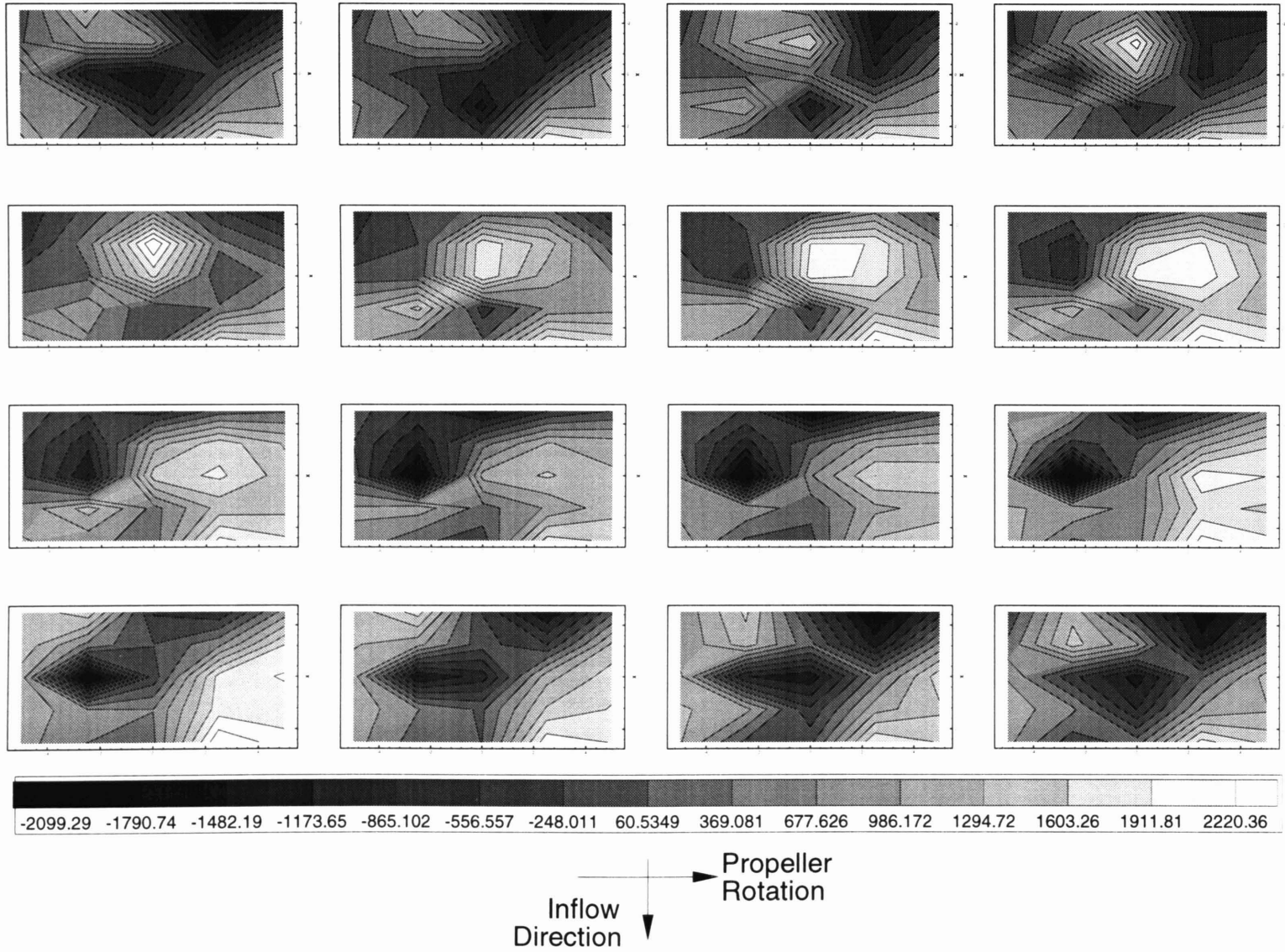


Figure 4-13: Tecplot^(R)Contour Plot for One Blade Passage of Run A

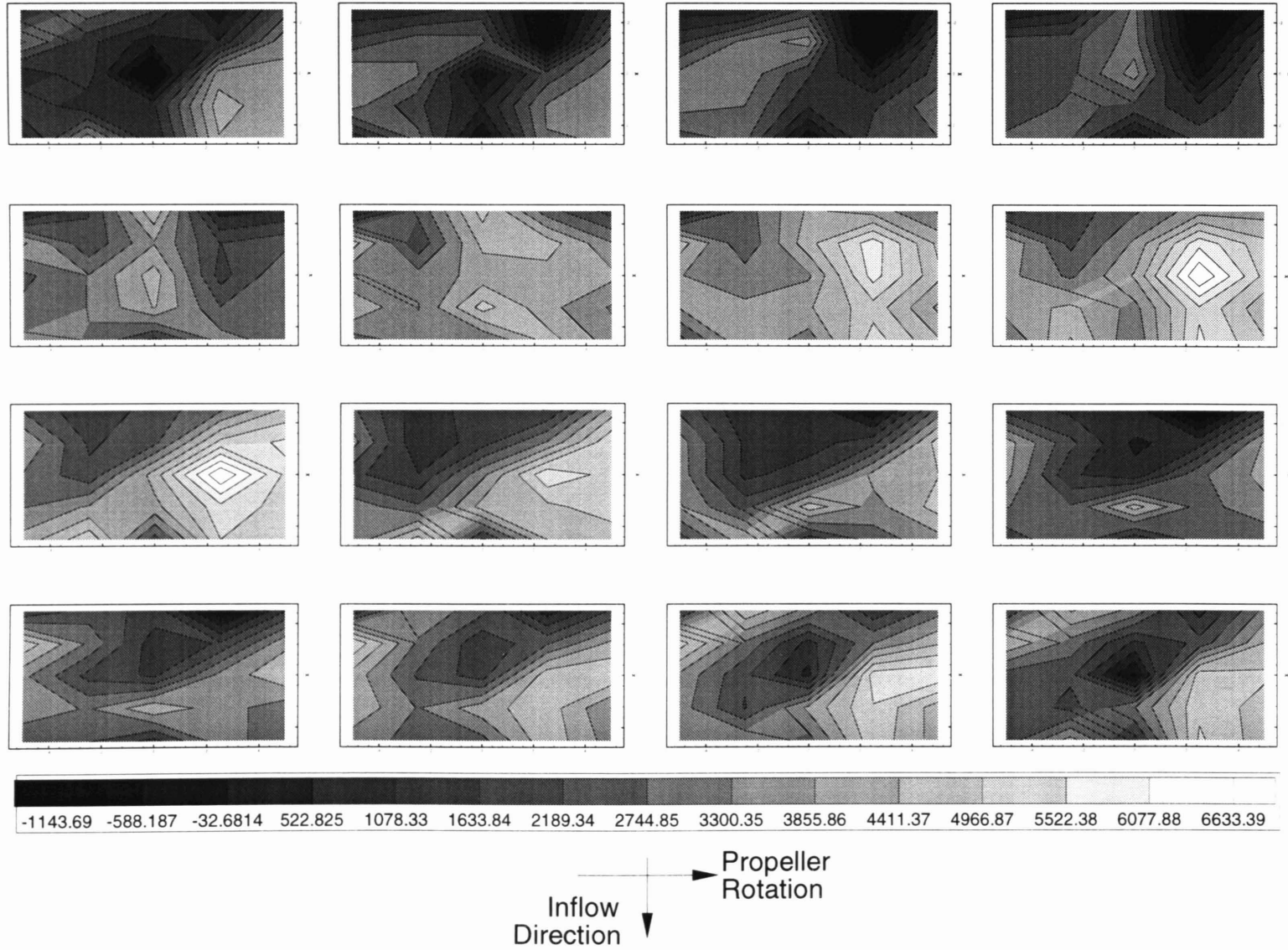


Figure 4-14: Tecplot^(R) Contour Plot for One Blade Passage of Run B

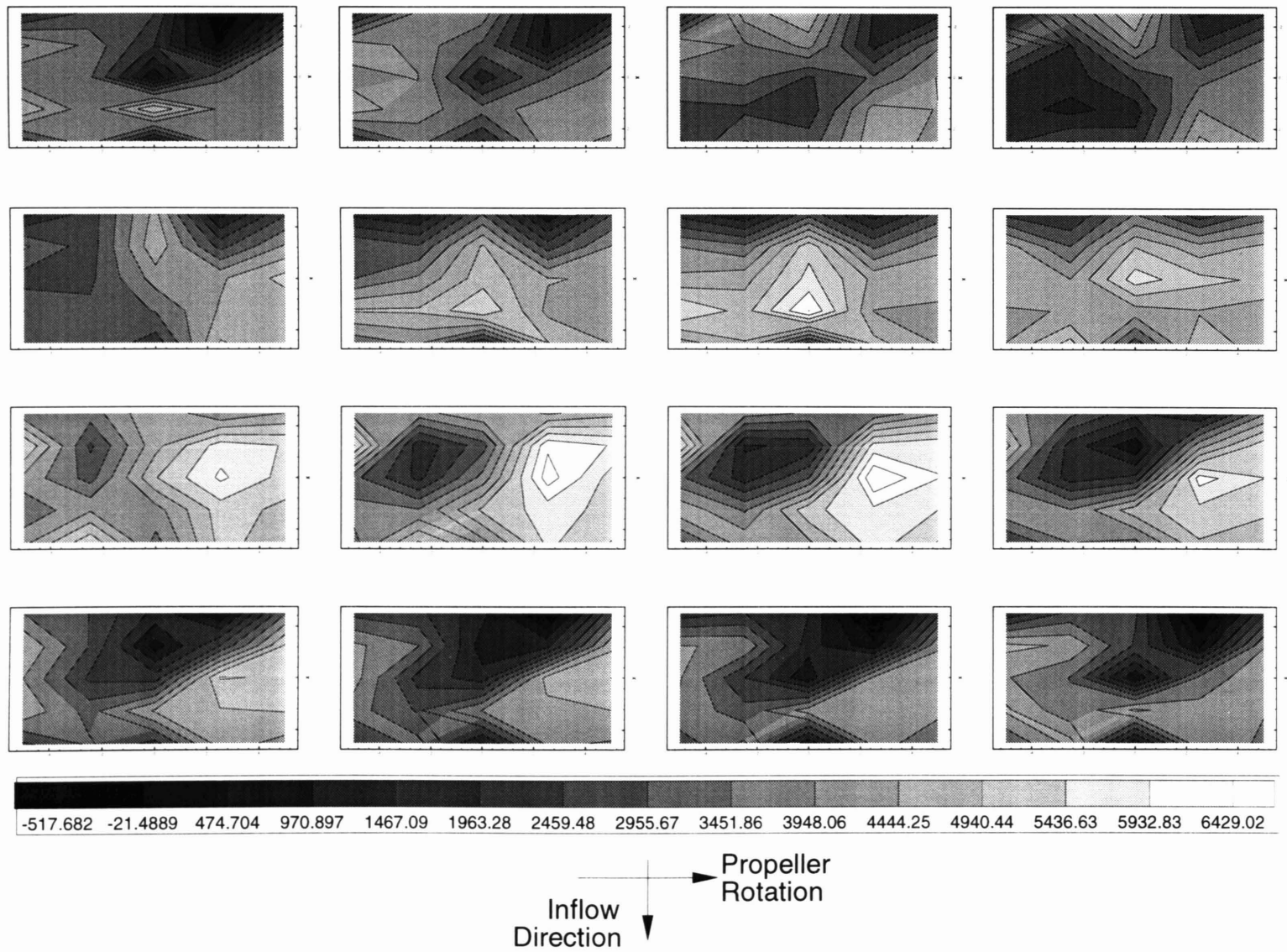


Figure 4-15: Tecplot^(R) Contour Plot for One Blade Passage of Run C

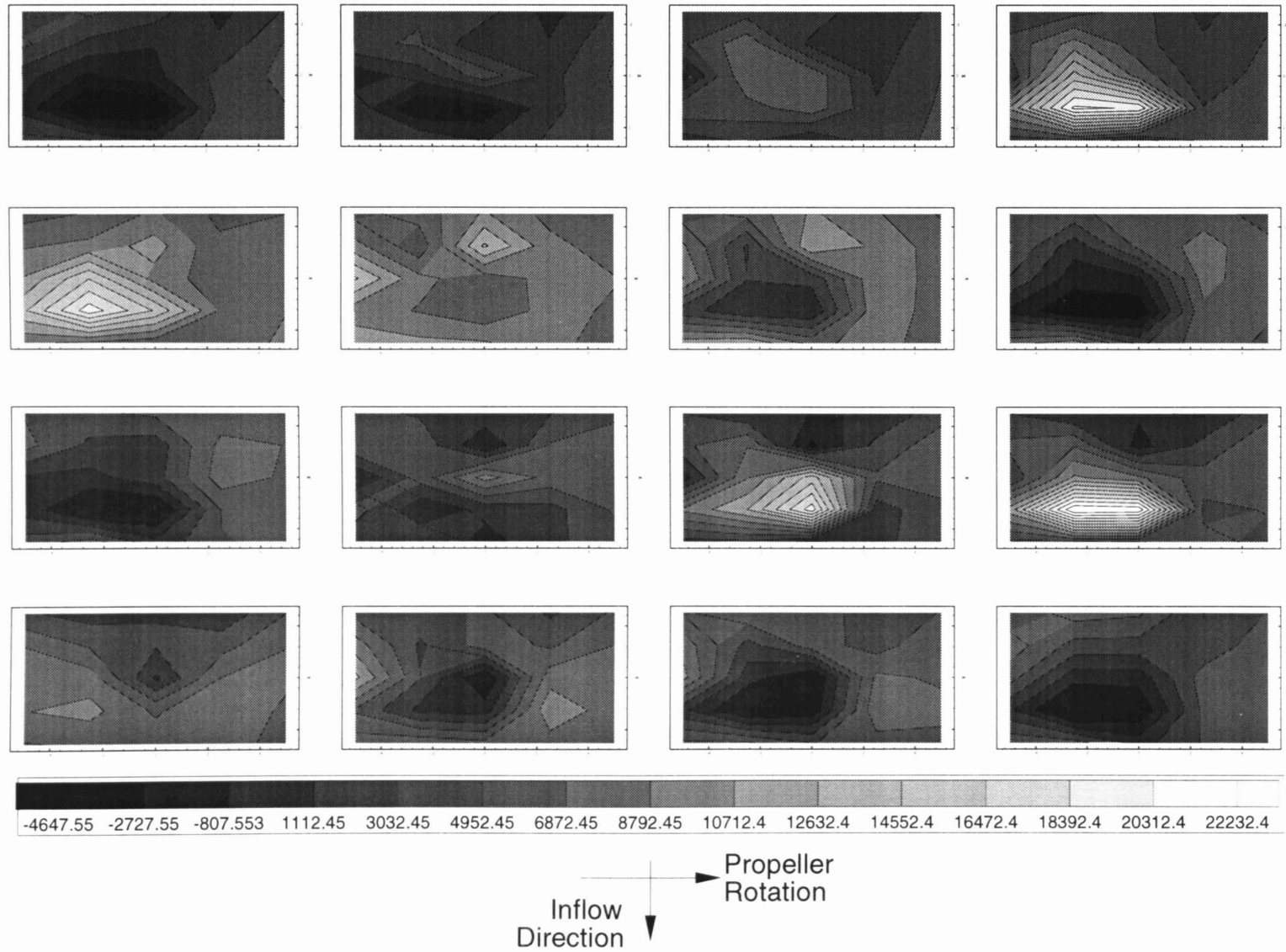


Figure 4-16: Tecplot^(R) Contour Plot for One Blade Passage of Run D

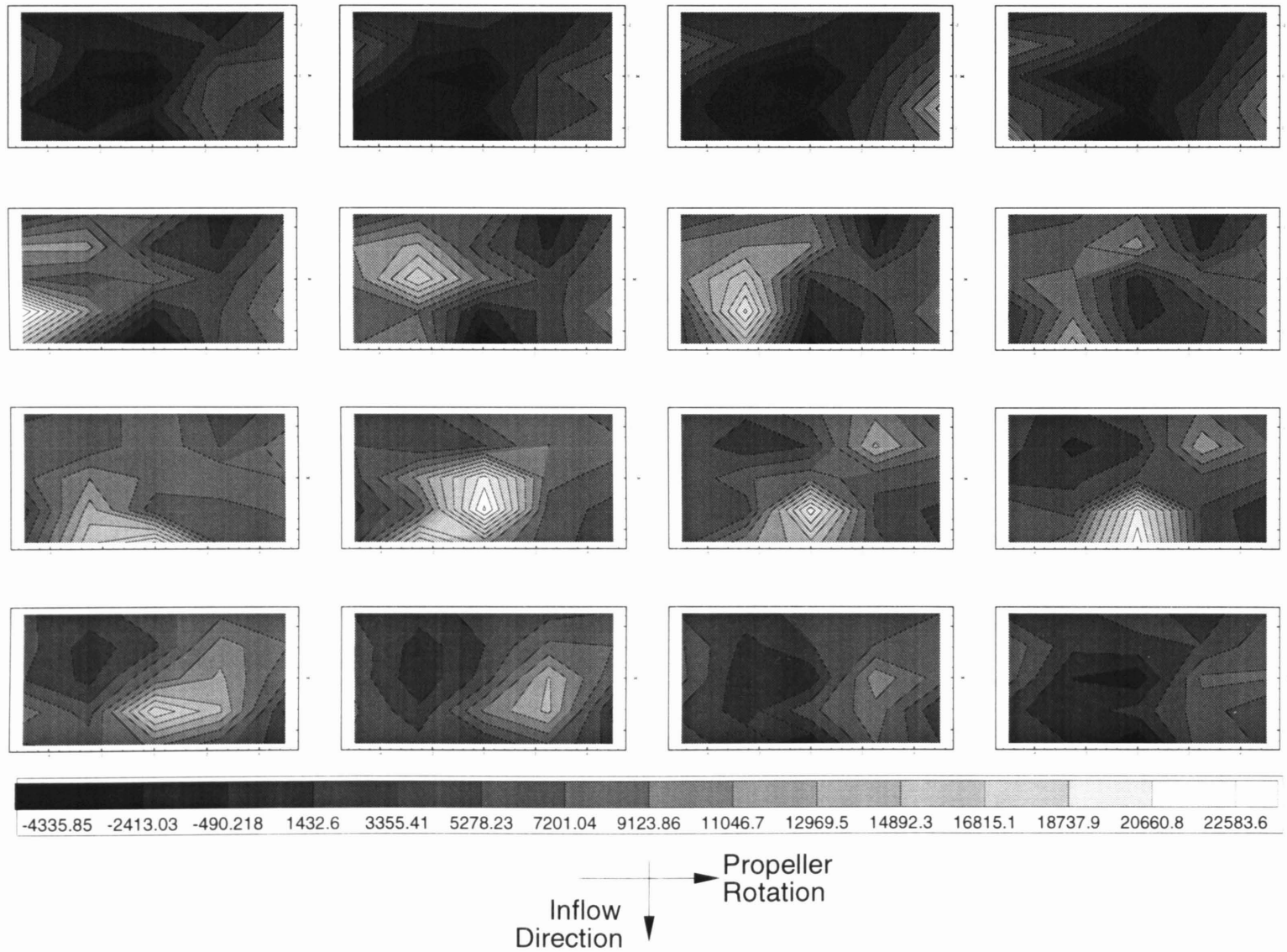


Figure 4-17: Tecplot^(R) Contour Plot for One Blade Passage of Run E

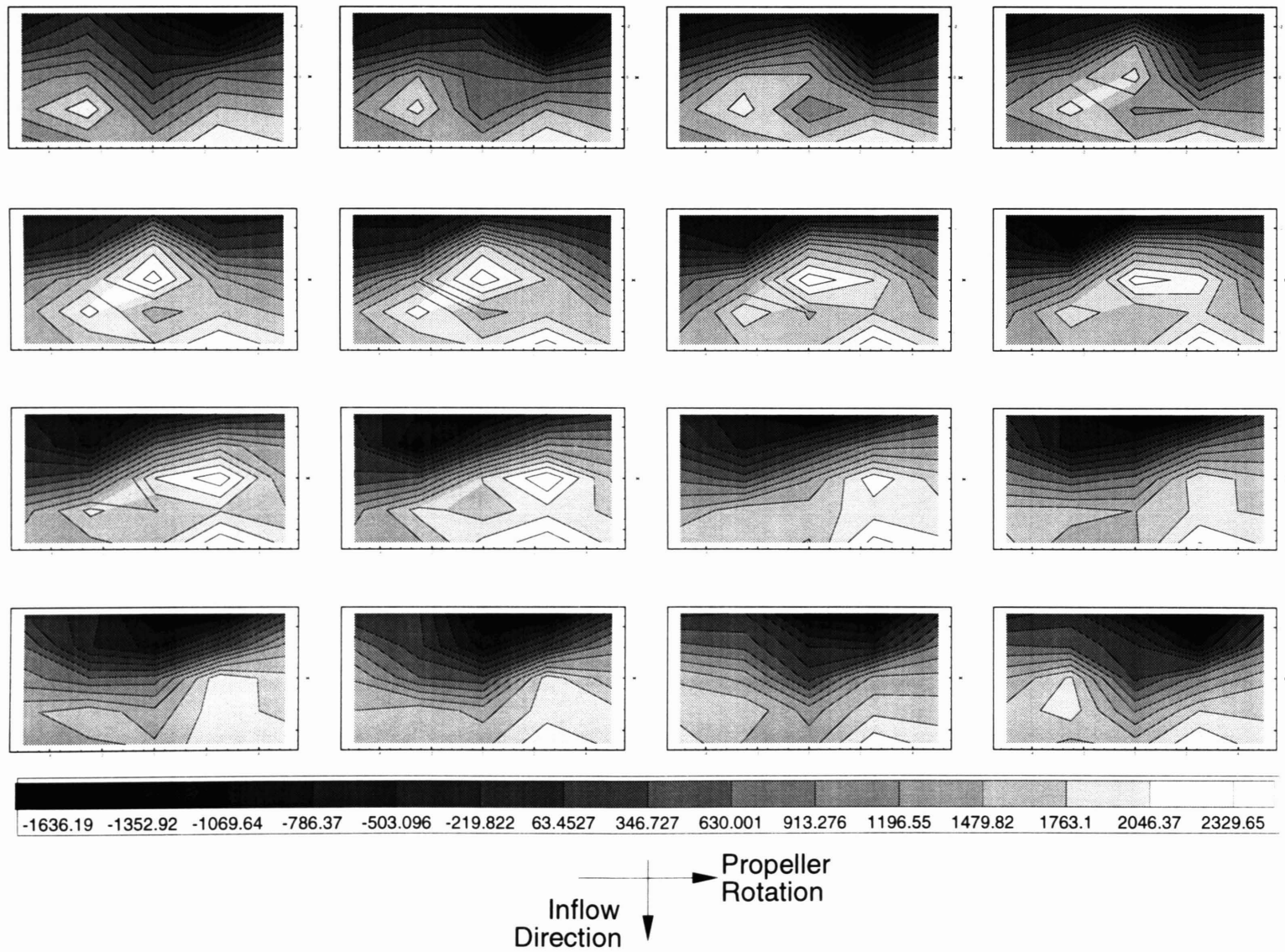


Figure 4-18: Tecplot^(R) Contour Plot for One Blade Passage of Run F

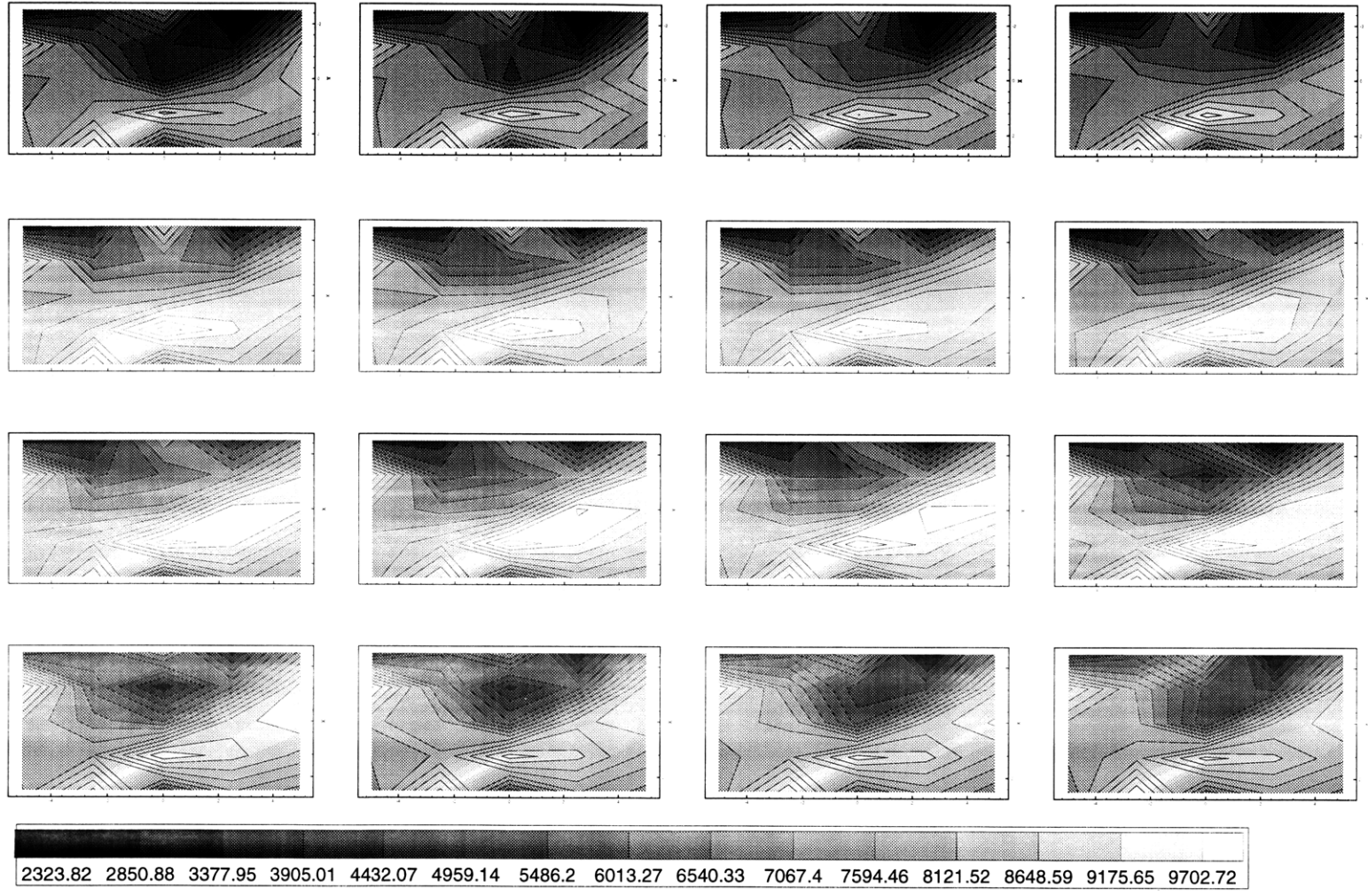


Figure 4-19: Tecplot^(R) Contour Plot for One Blade Passage of Run G

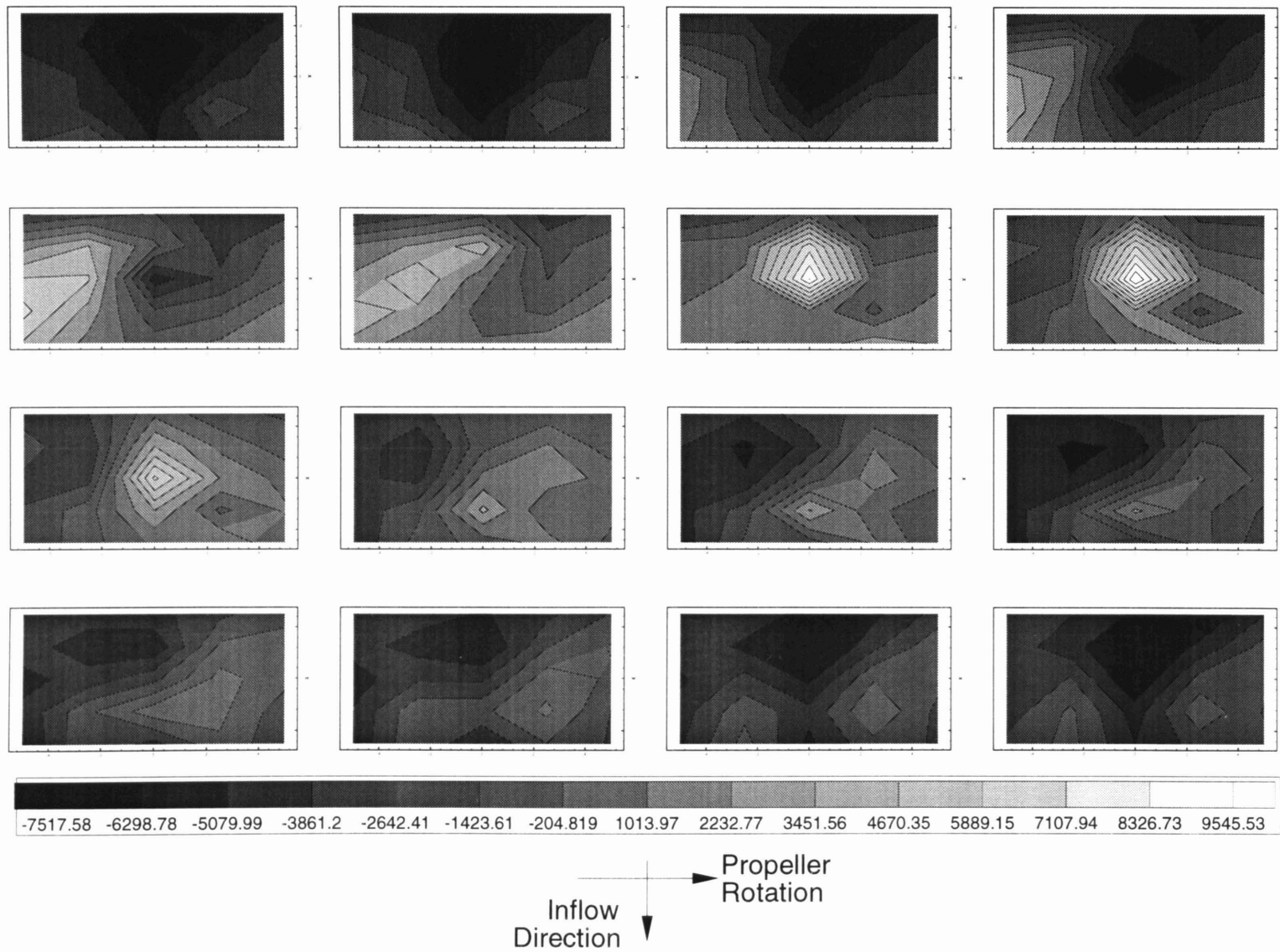


Figure 4-20: Tecplot^(R) Contour Plot for One Blade Passage of Run H

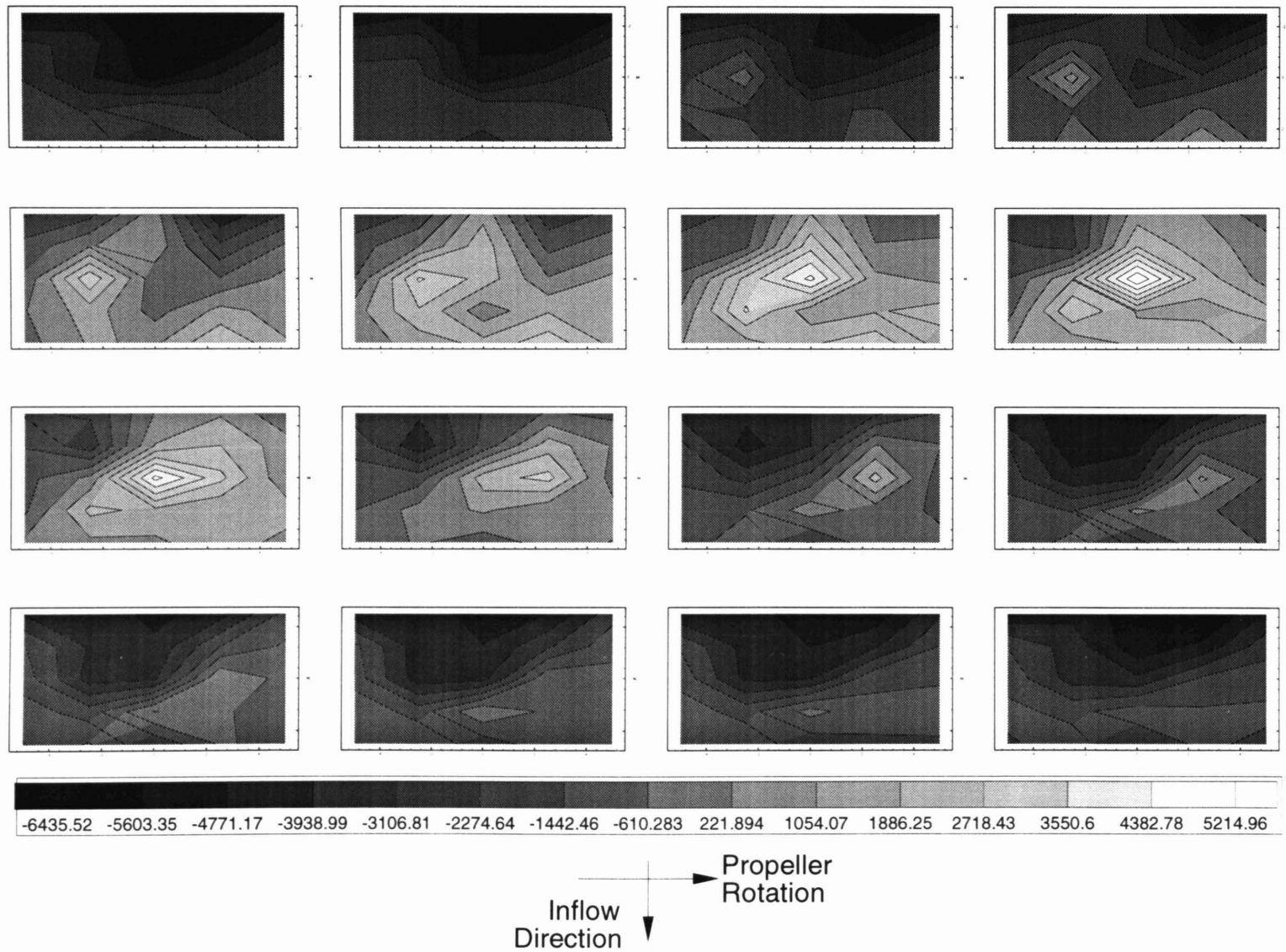


Figure 4-21: Tecplot^(R) Contour Plot for One Blade Passage of Run L

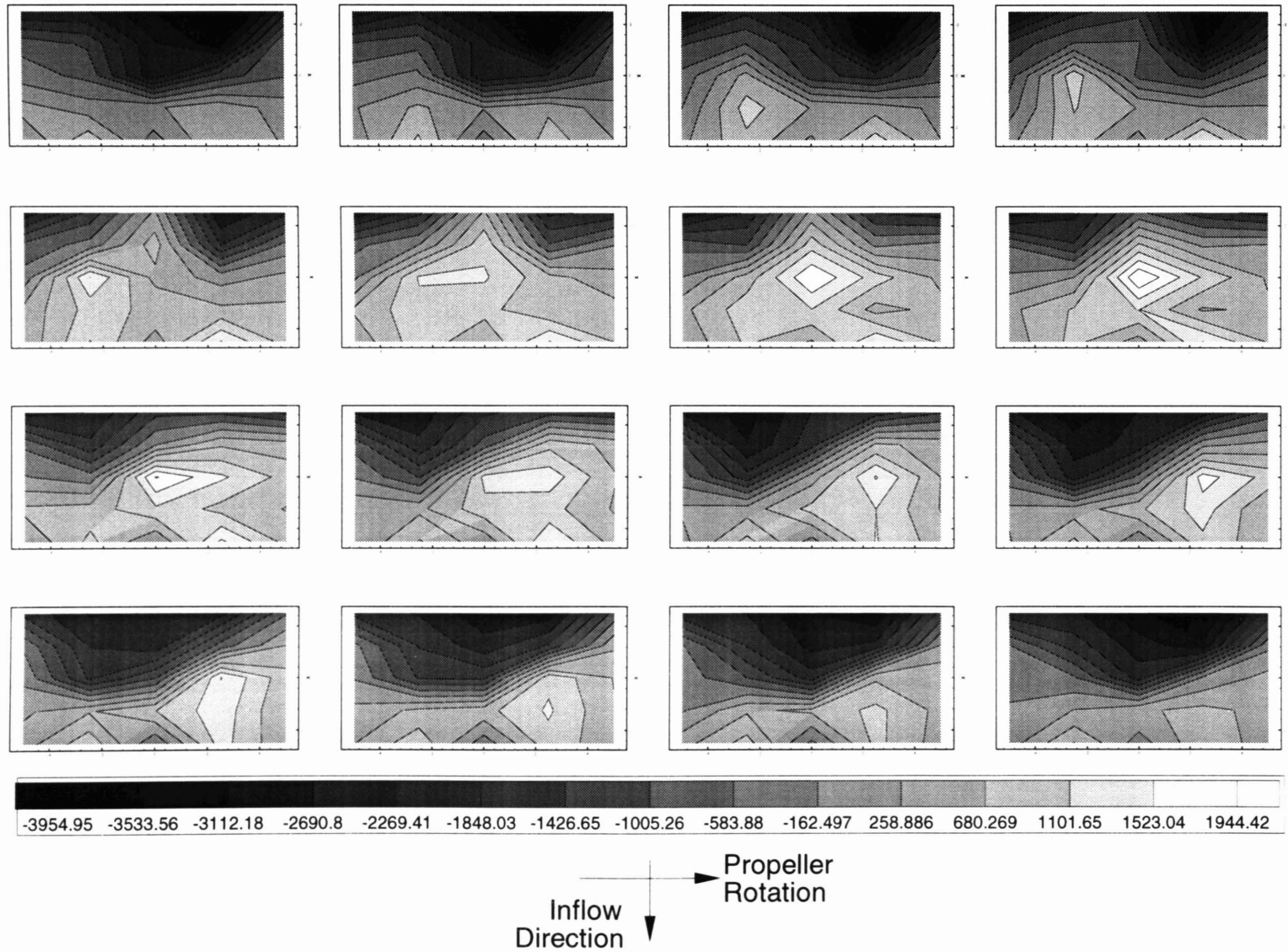


Figure 4-22: Tecplot^(R) Contour Plot for One Blade Passage of Run M

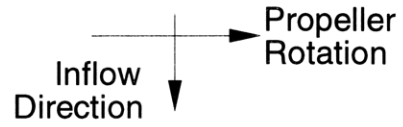
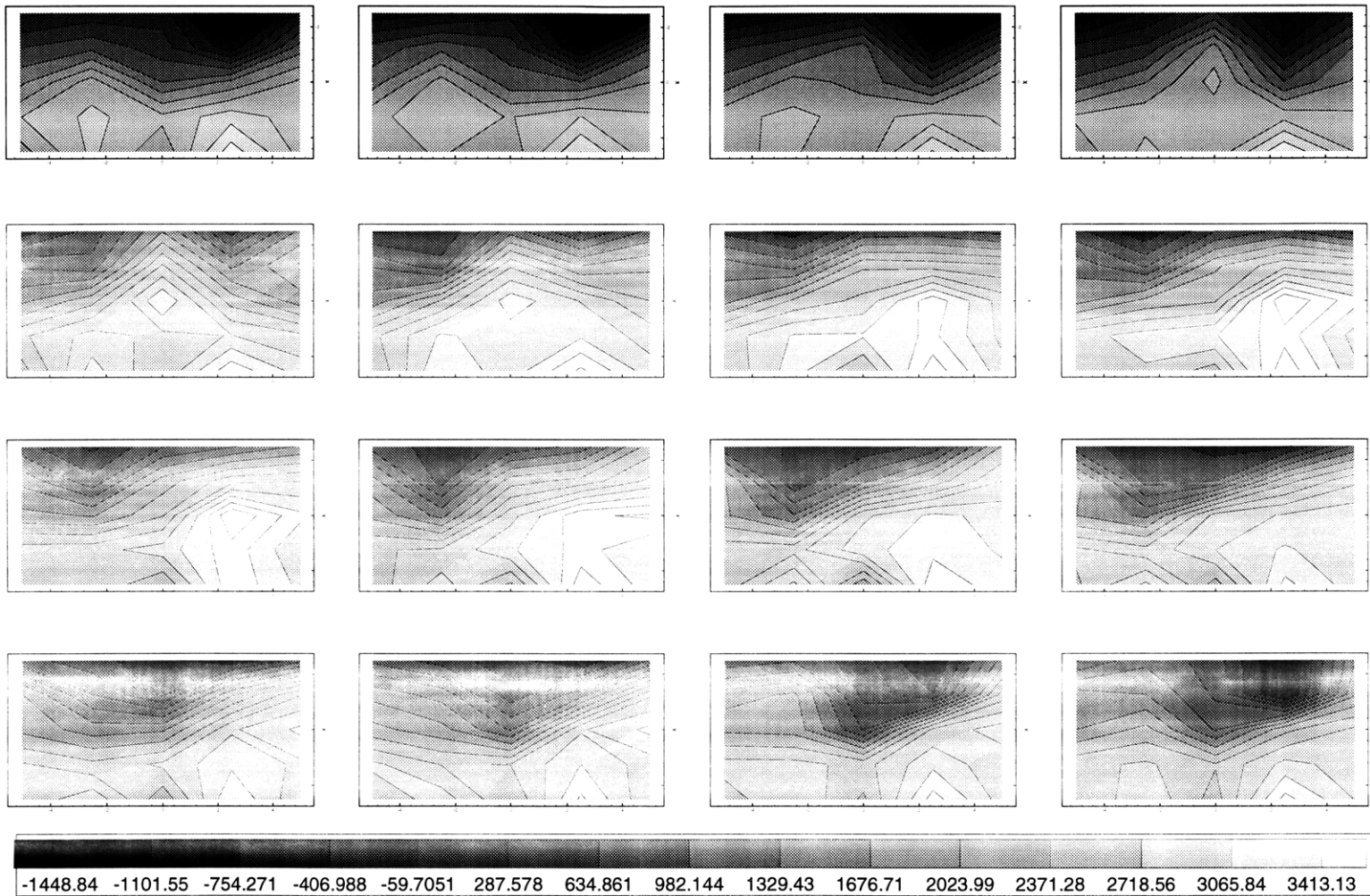


Figure 4-23: Tecplot^(R) Contour Plot for One Blade Passage of Run N

a single channel FFT on screen for a rough check. If the peaks of the FFT related to the frequency of blade passages, or 5 times the propeller rotation in Hz, then the dynamic pressures displayed the proper trends. The FFT analysis for each experimental run could be seen in appendix C.

4.3 Discussion and Improvements

4.3.1 Experimental Setup

The greatest, unnecessary difficulty in installing the experiment was plugging the pressure probes into the CX136-4 connectors. The connectors were designed to be attached to wires by a crimping method which was unreliable; therefore, the wires had to be soldered to the connectors. While soldering insured that the wire connections were strong, the solder interfered with the proper connection to the probes. Also, since the connectors were straight, rather than right angle connectors, the tension on the cables pulled on the probes during installation, making it slow and difficult. Instead of the CX136-4 connectors, a different 4-pin electrical connector should be found for this project. An additional modification that could make connecting the pressure probes easier would be to cut the aluminum strips to be as thin as possible, allowing the user to see the probe connection which was underneath the aluminum strips with this design.

Also, the hose connection from the PVC bladder to the water tunnel reference pressure should be reconsidered. At the completion of the experiment, a significant volume of water was emptied from the bladder. The water could have affected the calibration constants for the differential pressure probes. The setup of the bladder connections should have kept the bladder dry, but the water probably traveled across the tunnel reference hose into the bladder. In later incarnations of this experiment, this reference should be checked and perhaps a different reference point should be used.

While this experiment was designed specifically for testing the cavitation of the 4842 propeller, the system could be used for testing any propeller. To lower the aluminum plate into the test section for a smaller propeller, a flat spacer plate with cut-out sections, similar to the plexiglass window, could be made to separate the aluminum plate from the window and still leave the pressure probe connection points dry on the outside.

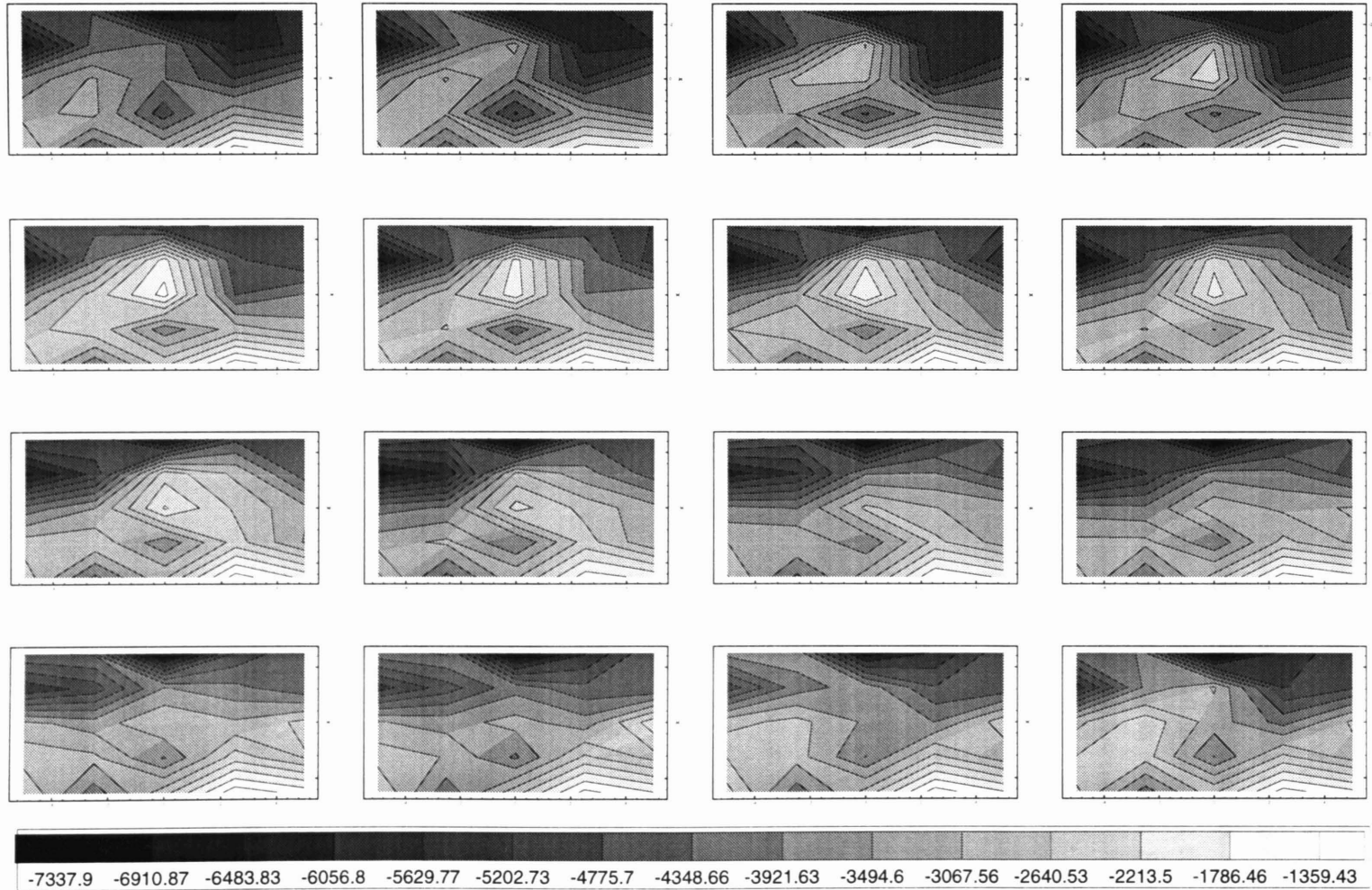


Figure 4-24: Tecplot^(R) Contour Plot for One Blade Passage of Run O

4.3.2 Experimental Program

After the completion of these experimental runs, the TestPointTM application, *Experiment*, was found to have a couple of typos. These typos appear in the section of the program which places data into container objects for storage. These typos caused questions about how well the program used the method of storing data in containers, but the FFT analysis of the full data sets (in appendix C) support the output data as correct. For future use of the experimental apparatus and applications, the error was corrected.

Appendix A

Two-Dimensional Foil Cavitation Experiment

At the beginning of the CAPREX IV project, a great deal of interest was directed at the incidence of bubble cavitation and its relationship to other cavitation types—specifically midchord cavitation. Two particular studies were found and used as a background for an in-house two-dimensional bubble cavitation study. The first study, [3], dealt with the relationship of bubble cavitation and other types of cavitation. From two-dimensional tests performed on a single foil for [3], a map of cavitation type versus both cavitation number and angle of attack was created. The map included the cavitation bucket as well as leading edge sheet, midchord sheet, and bubble cavitation regimes. One other important aspect of the [3] study was the change in the cavitation map with the total absence of gas nuclei. The second study, detailed in [9] and [8], related the presence of sheet and bubble cavitation on smooth and rough propeller blades at different advance coefficients with and without nuclei added to the water. Along with providing discussion about bubble cavitation on a three-dimensional propeller, [9] and [8] only found bubble cavitation at the midchord of the propeller blade.

An observational experiment was performed of the HRA two-dimensional foil studied in [5] in the Water Tunnel as an attempt to test and understand the cavitation map found in [3]. The cavitation map created from the HRA tests, figure A-1, showed strong similarities to the [3] map. The fact that the experimental cavitation map showed the same trend of change from leading edge sheet cavitation to midchord cavitation to bubble cavitation for decreasing cavitation number at high enough angle of attack, supported the theory that the cavitation types had strong relationships. The relatively flat pressure distribution for both the [3] foil and the HRA foil called into question the direct relationship between the changes

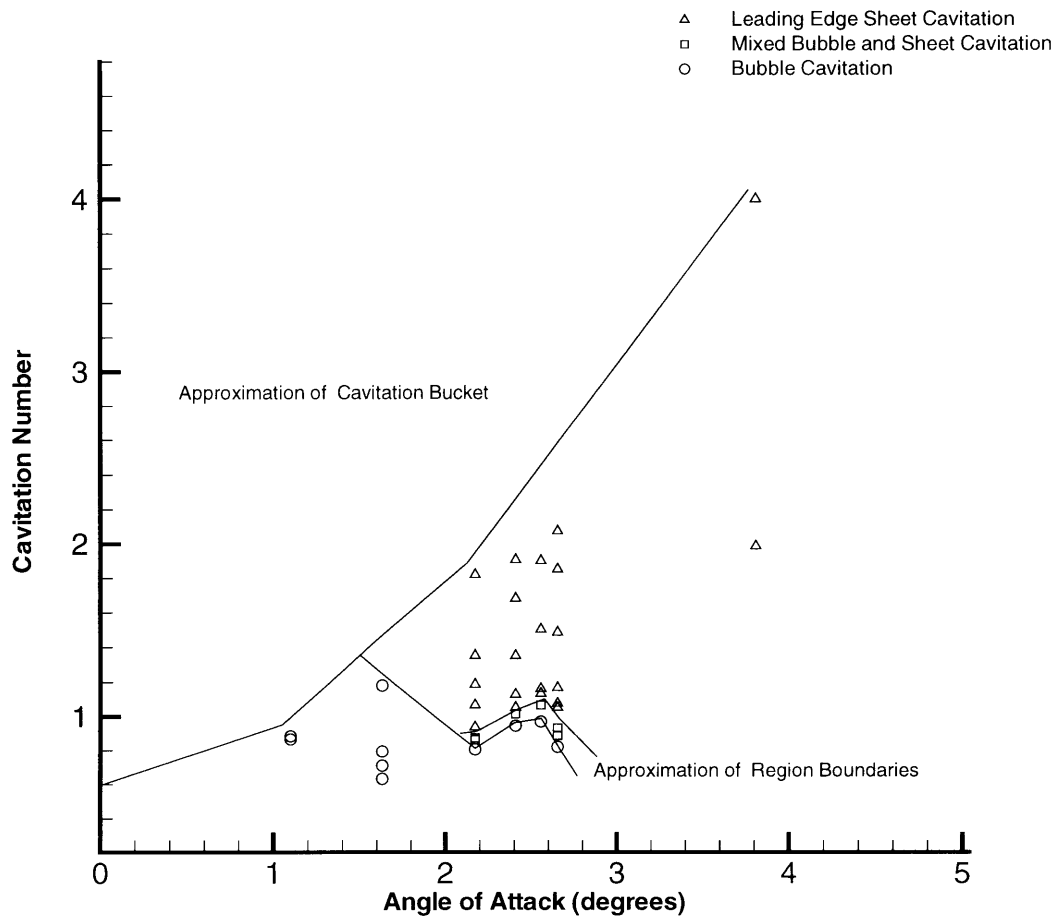


Figure A-1: Experimental Cavitation Map for the HRA Two-Dimensional Foil

on the cavitation map and the changes in the pressure distribution with the angle of attack. A more detailed study would need to be performed to elaborate on that relationship.

The section of the [3] cavitation map referred to as the "Mixed cavitation band" or in figure A-1 as the "Mixed Bubble and Sheet Cavitation Regime" raised questions about the relationship between sheet cavitation and bubble cavitation. In that cavitation regime, a sheet cavity appeared to pulse back and forth on the foil – sweeping onto and off of the foil surface. When the sheet cavity moved off of the surface, it would be replaced with bubble cavitation. The dynamic relationship between the two cavitation types has been theorized to be affected by the change in laminar separation caused by each of the two cavitation types. This also would need to be studied further to understand the true dynamic situation.

In both studies, the influence of gas nuclei was looked at. In [3], a cavitation map was created for the foil with no nuclei seeding. The resulting map had a wider cavitation bucket which showed no cavitation for any cavitation number at and around a 4° angle of attack. Also, what was bubble cavitation on the nuclei included map was a full span, midchord sheet on the no-nuclei map. The conclusions from [9] and [8] also state a strong dependence of bubble cavitation inception on gas nuclei content. These studies found that roughness on the leading edge of the propeller blade created sufficient gas nuclei to incept bubble cavitation. The sheet cavitation on the propeller blades was, however, not found to be dependent on the gas nuclei. Since the Water Tunnel could not count or control gas nuclei, this aspect of the bubble cavitation could not be explored.

The HRA foil tests did reveal a very important aspect of bubble cavitation studies – visualization. When the HRA foil was cavitating at the correct cavitation number and angle of attack to see bubble cavitation, the naked eye could only see turbulent cavitation on the foil. Only with the aid of a strobe light or a high speed camera, could the very distinct bubble formations be seen. This was best explained through photographs of the HRA foil tests taken at different shutter speeds. In figure A-2 with the camera shutter speed at $\frac{1}{2000}th$ of a second, the separate bubbles that appeared on the foil surface could be seen, while in figure A-3 the shutter speed was only $\frac{1}{500}th$ of a second and the cavitation looked more like streaks of turbulence or a turbulent sheet cavitation layer. The particular lesson from these figures was that bubble cavitation would need to be visualized with a strobe light to correctly identify the cavitation type.

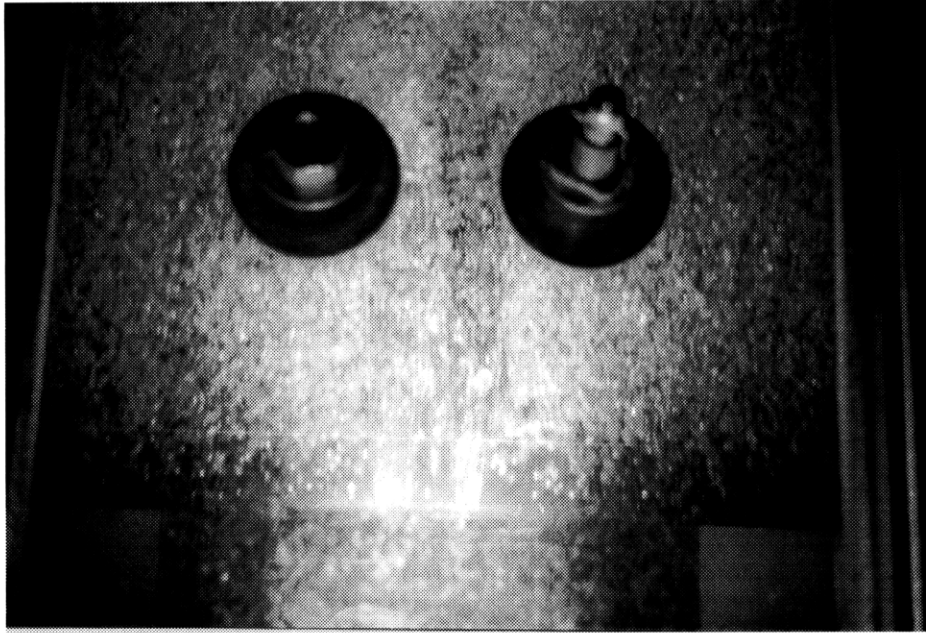


Figure A-2: Photograph of Bubble Cavitation on the HRA Two-Dimensional Foil at Cavitation Number $\sigma = 0.488$ and Angle of Attack $\alpha = 2^\circ$ with Camera Shutter Speed at $\frac{1}{2000}$ seconds

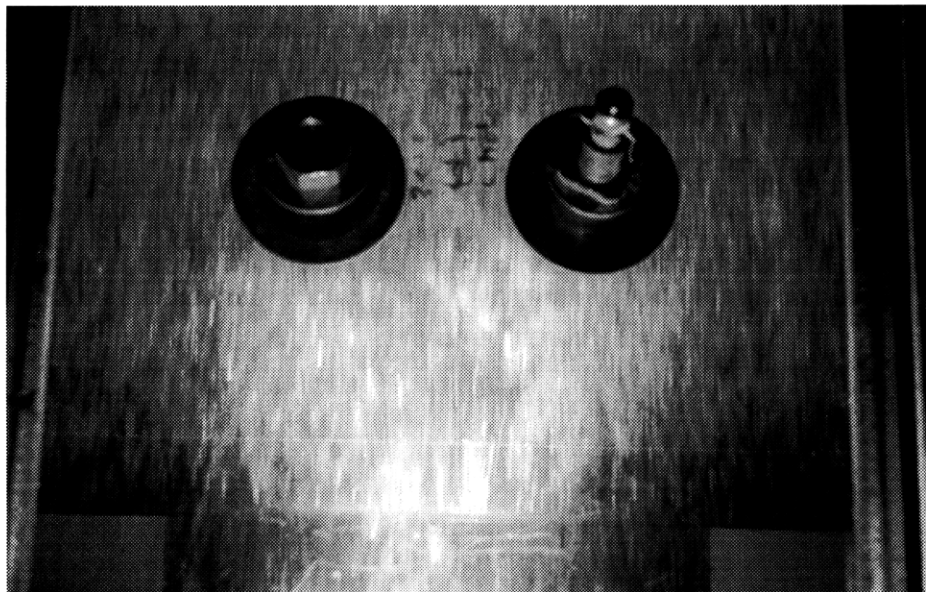


Figure A-3: Photograph of Bubble Cavitation on the HRA Two-Dimensional Foil at Cavitation Number $\sigma = 0.488$ and Angle of Attack $\alpha = 2^\circ$ with Camera Shutter Speed at $\frac{1}{500}$ seconds

Appendix B

Fortran and Matlab Programs

B.1 Matlab Calibration Program

```
load calibration.dat
[r c]=size(calibration);
height=calibration(1,1:c);
channel=calibration(2:r,1:c);
clear calibration

atmospheric=758.25;
atmosPa=atmospheric*10000/760;

rho=997;
g=9.8038;
height=height./100;
pressure=rho*g.*height;
pressuregauge=pressure + atmosPa;

for i=1:r-2
    constants(i,1:2)=polyfit(channel(i,1:c),pressure,1);
end
    constants(r-1,1:2)=polyfit(channel(r-1,1:c),pressuregauge,1);

save calibconstants.dat constants -ascii
```

B.2 Fortran Post-Processing Program

```

CCCCCCCCCCCCCCCCCCCCCCCCCCCCCCCCCCCCCCCCCCCCCCCCCCCCCCCCCCCCCCCC
C
C          Program to take CAPREX IV pressure data and          C
C          create Tecplot Data files for IJK movies of          C
C          output at a variable time                            C
C                                                                 C
CCCCCCCCCCCCCCCCCCCCCCCCCCCCCCCCCCCCCCCCCCCCCCCCCCCCCCCCCCCCCCCC

      PROGRAM CAPREX

      real calib(0:28,2)
      real output(0:28,20000)
      integer itry,i,j,k,t
      CHARACTER*30 MFNAME,NAME,TECNAME

!.....Open file and read it
      ITRY=0
101  WRITE(*,'(A)',ADVANCE='NO')
      *          '      Enter data file name...      '
      READ(*,'(A)') MFNAME
      OPEN(15,FILE=MFNAME,STATUS='OLD',ERR=111,FORM='FORMATTED')
      write(*,*)"
      GO TO 121
111  CONTINUE
      ITRY=ITRY+1
      IF(ITRY==5 .OR. MFNAME=='quit' .OR. MFNAME=='exit') STOP
      WRITE(*,'(A)') ' !!! File not found. Try again !!! '
      GO TO 101
121  continue

      write(6,*) '      ... reading data ...'

      DO i=1 , 20000
          read(15,*) ( output(j,i) , j=0,29)
      enddo

!.....Use calibration constants to make output in pressure

      write(6,*) '      calibrating data'

      OPEN(14,FILE='calibconstants.dat',status='old',form='formatted')
      Do j=0,28
          read(14,*) ( calib(j,k) , k=1,2)
      enddo

      Do j=0,28
          Do i=1,20000
              output(j,i)=output(j,i)*calib(j,1) + calib(j,2)
          enddo
      enddo

```

```

    Do j=0,26
      Do i=1,20000
        output(j,i)=output(j,i) - output(27,i)
      enddo
    enddo

!.....Open and write to output file
  ITRY=0
201 WRITE(*,'(A)',ADVANCE='NO')
  *           '      Enter tecplot file name (.dat)...      '
  READ(*,'(A)') TECNAME

  OPEN(16,FILE=TECNAME,STATUS='NEW',ERR=211)
  write(*,*)""
  GO TO 221
211 CONTINUE
  ITRY=ITRY+1
  IF(ITRY==5 .OR. MFNAME=='quit' .OR. MFNAME=='exit') STOP
  WRITE(*,'(A)') ' !!! File already exists. Try another name !!! '
  GO TO 201

221 continue

  write(6,*) '    ... writing Tecplot files ...'

  WRITE(16,*)'TITLE=""',MFNAME,'"'
  WRITE(16,*)'VARIABLES="X" "Y" "OUTPUT"'
  WRITE(16,*)'ZONE I=5 J=5 K=1800 F=POINT'

  DO t=1,1800
    DO i=1,5
      DO j=1, 5
        y=-5.0+(j-1)*2.5

        x=-2.50+(i-1)*1.25
        iout=(i-1)*5+j
        write(16,*) x, y, output(iout,t)

      enddo
    enddo
  enddo

end

```

Appendix C

FFT Analysis of Dynamic Pressure Measurements

Each experimental run's data was analyzed to extract the primary frequency of the dynamic pressures. Each primary frequency should match the frequency of blade passage for that run. With this five bladed propeller, the expected output value should be the rotational speed per second divided by 5 or

$$\frac{\text{Propeller rpm} \cdot \left(\frac{1 \text{ minute}}{60 \text{ seconds}}\right)}{5 \text{ blades}} = \text{Blade Passage Frequency, Hz.}$$

That expected value was compared to the primary frequency found from a power spectrum analysis of the data set for the center probe of the 5×5 array, channel 13, using the Matlab spectrum function. The power spectrum output, with the primary frequencies highlighted, was graphed in figures C-1 through C-12.

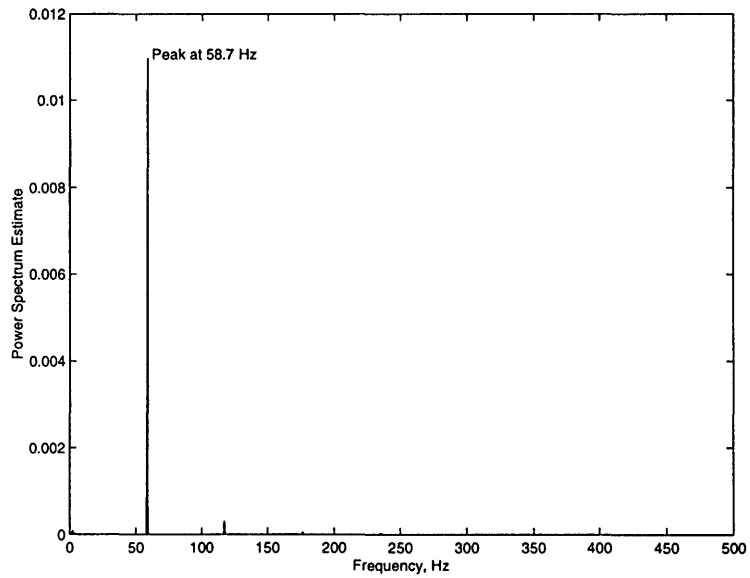


Figure C-1: FFT Analysis for Run A, Blade Passage Frequency at 58.9 Hz

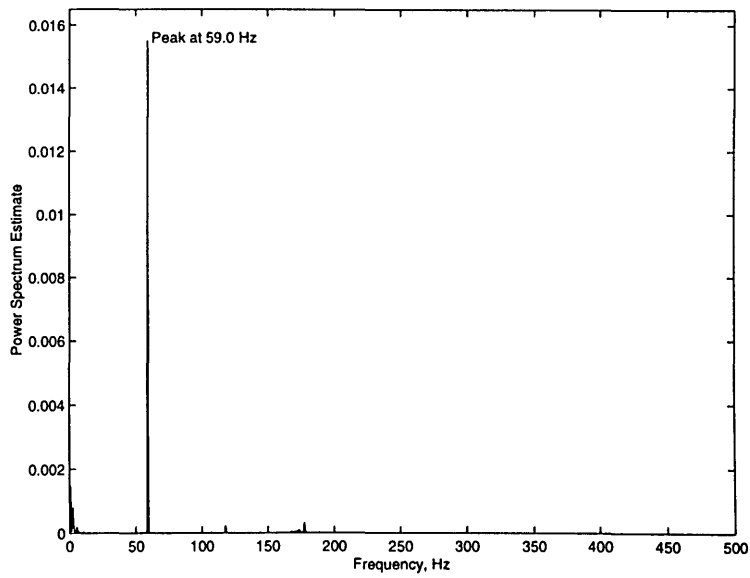


Figure C-2: FFT Analysis for Run B, Blade Passage Frequency at 59.0 Hz

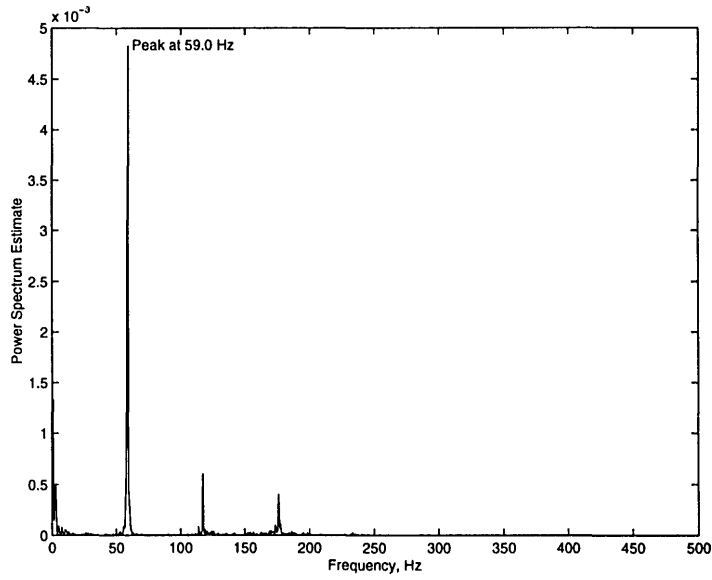


Figure C-3: FFT Analysis for Run C, Blade Passage Frequency at 58.7 Hz

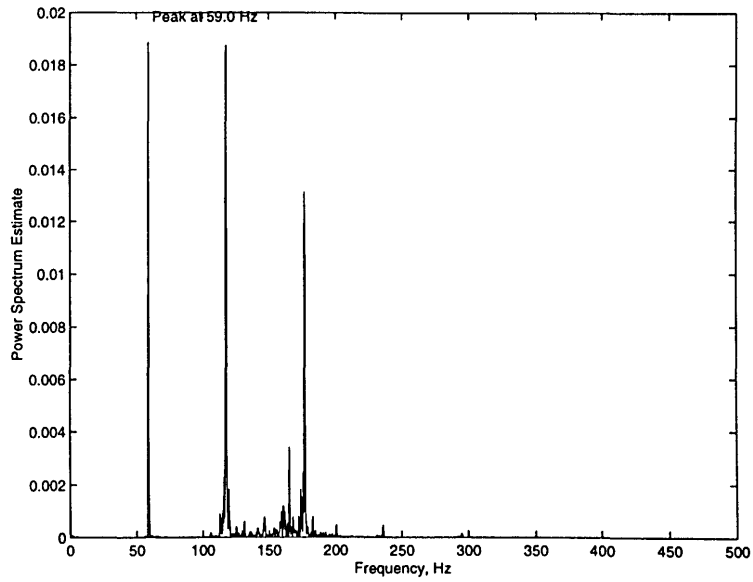


Figure C-4: FFT Analysis for Run D, Blade Passage Frequency at 58.8 Hz

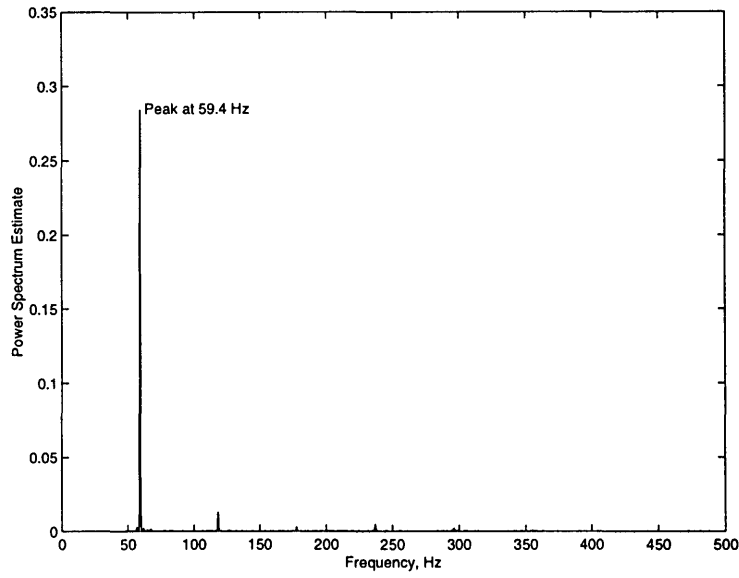


Figure C-5: FFT Analysis for Run E, Blade Passage Frequency at 58.7 Hz

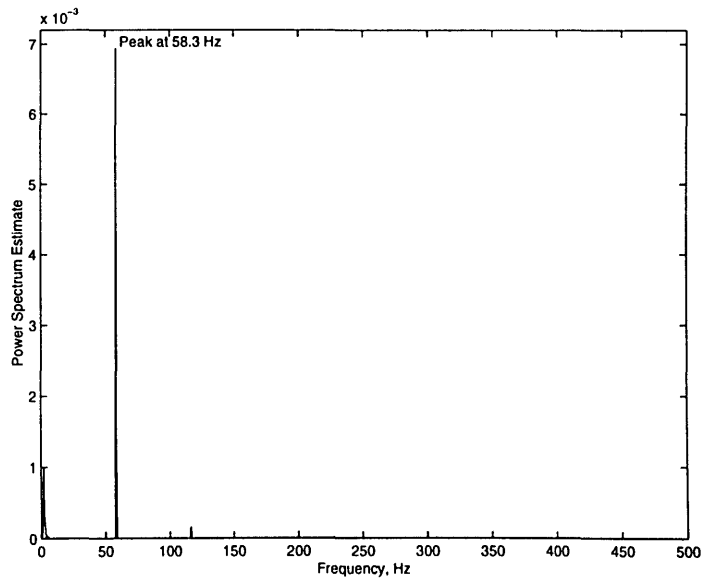


Figure C-6: FFT Analysis for Run F, Blade Passage Frequency at 58.3 Hz

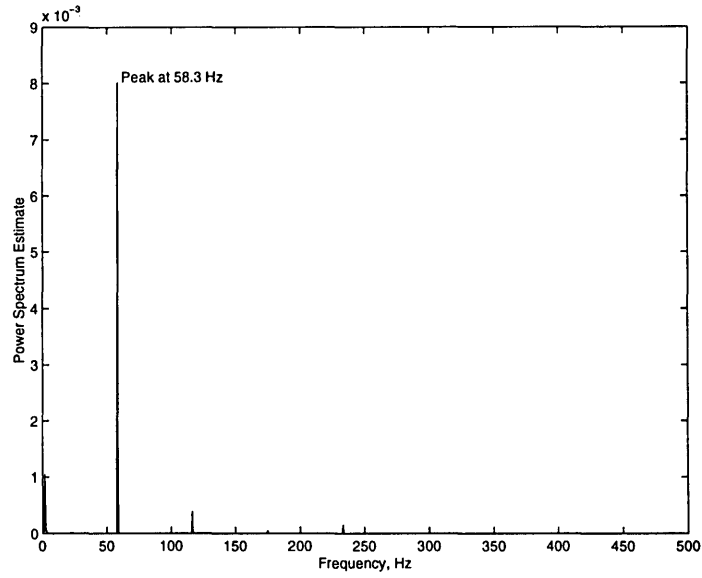


Figure C-7: FFT Analysis for Run G, Blade Passage Frequency at 58.3 Hz

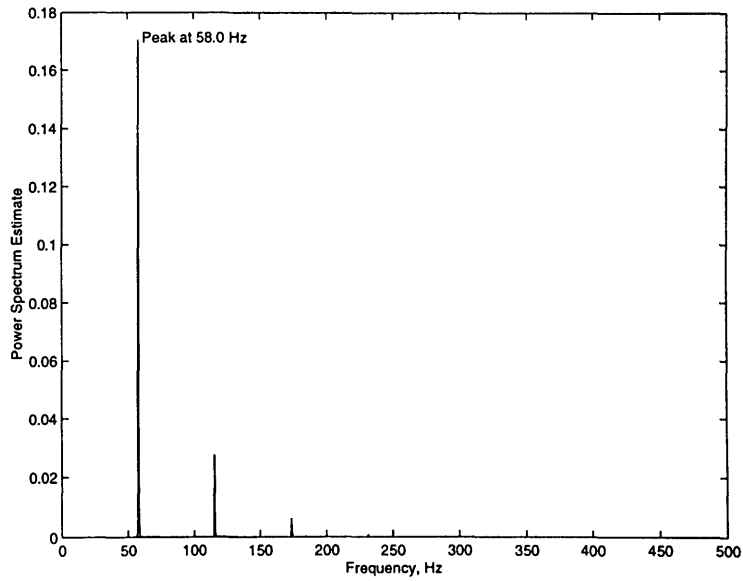


Figure C-8: FFT Analysis for Run H, Blade Passage Frequency at 57.9 Hz

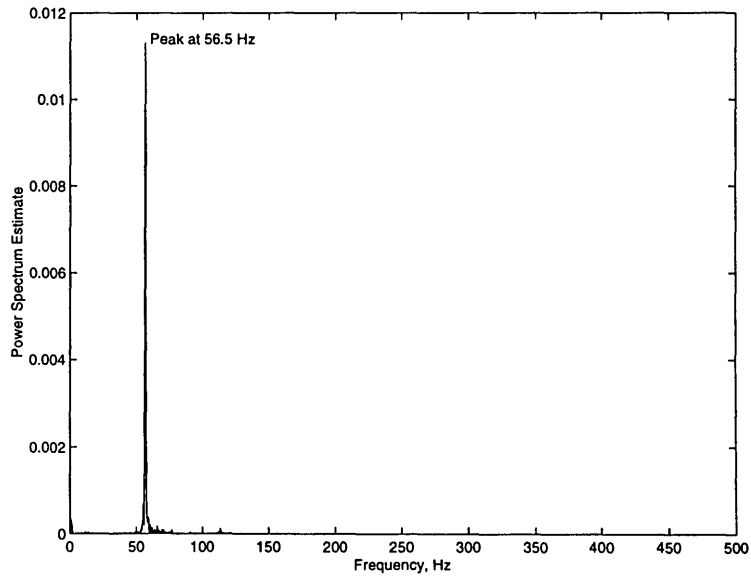


Figure C-9: FFT Analysis for Run L, Blade Passage Frequency at 57.1 Hz

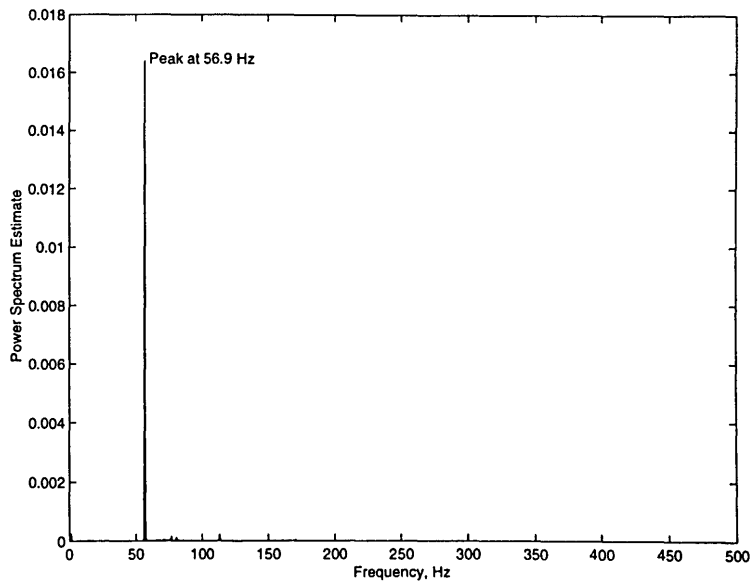


Figure C-10: FFT Analysis for Run M, Blade Passage Frequency at 56.9 Hz

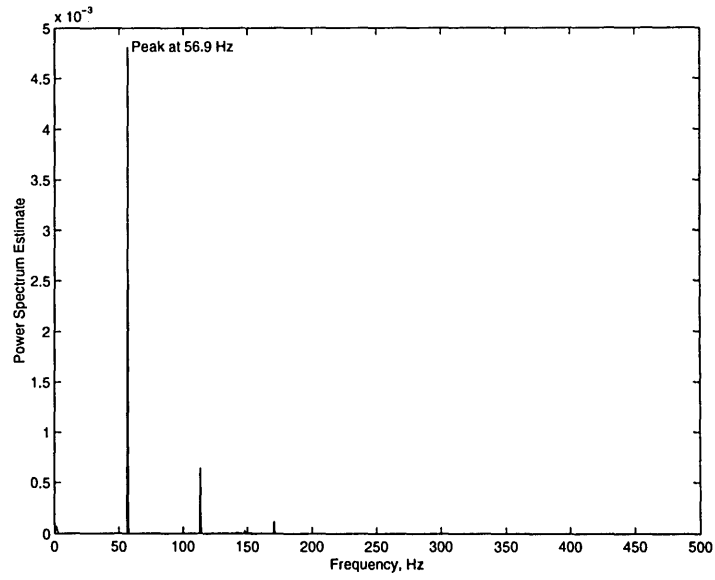


Figure C-11: FFT Analysis for Run N, Blade Passage Frequency at 56.9 Hz

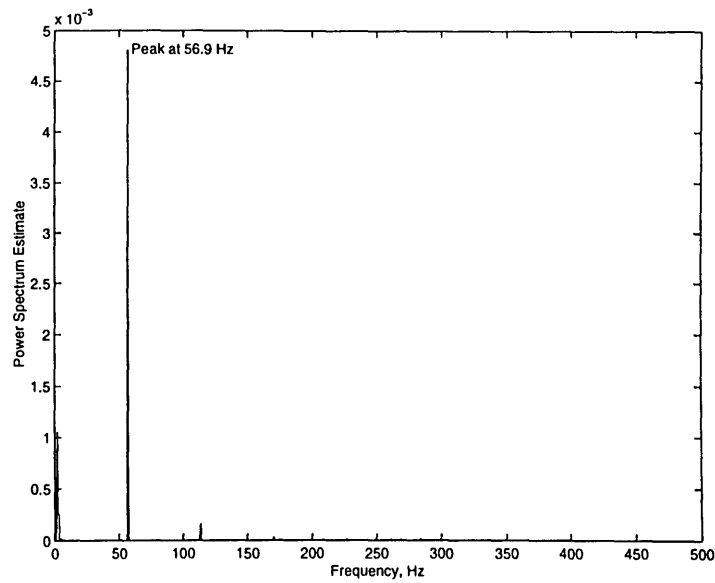


Figure C-12: FFT Analysis for Run O, Blade Passage Frequency at 56.8 Hz

Bibliography

- [1] William K. Blake, K. Meyne, J. E. Kerwin, E. Weitendorf, and J. Friesch. Design of APL C-10 Propeller with Full-Scale Measurements and Observations Under Service Conditions. *SNAME Transactions*, 1990.
- [2] J. P. Breslin, R. J. Van Houten, J. E. Kerwin, and C-A. Johnsson. Theoretical and Experimental Propeller-Induced Hull Pressures Arising from Intermittent Blade Cavitation, Loading and Thickness. *SNAME Transactions*, 90, 1982.
- [3] L. Briancon-Marjollet, J. P. Franc, and J. Michel. Transient Bubbles Interacting with an Attached Cavity and the Boundary Layer. *Journal of Fluid Mechanics*, 218, 1990.
- [4] Capital Equipment Corporation, Billerica, Massachusetts. *TestPoint User's Guide: Techniques and Reference*, 1996.
- [5] Bruce D. Cox, Richard W. Kimball, and Otto Scherer. Hydrofoil Sections With Thick Trailing Edges. In *Propeller/Shafting '97 Symposium*, Virginia Beach, VA, September 1997. The Society of Naval Architects and Marine Engineers.
- [6] Keithley MetraByte Division, Keithley Instruments, Inc., Taunton, Massachusetts. *DAS-1800HC Series User's Guide*, 1995.
- [7] Richard W. Kimball. Measurement of the Unsteady Pressure Field Induced on a Wall by a Cavitating Propeller. Technical report, Massachusetts Institute of Technology, Department of Ocean Engineering, 1997.
- [8] G. Kuiper. Some Experiments With Distinguished Types of Cavitation on Ship Propellers. In *International Symposium on Cavitation Inception*, pages 171–205, New York, NY, December 1979. ASME Winter Annual Meeting.
- [9] G. Kuiper. Some Experiments With Specific Types of Cavitation on Ship Propellers. *Journal of Fluids Engineering, Transactions of the ASME*, 1982.

- [10] Shigenori Mishima. *Design of cavitating propeller blades in non-uniform flow by numerical optimization*. PhD thesis, Massachusetts Institute of Technology, Department of Ocean Engineering, 1996.
- [11] John Nichols Newman. *Marine Hydrodynamics*. The MIT Press, Cambridge, Massachusetts, 1992.